Science Advances
AAAS

Supplementary Materials for

Chromosome architecture affects virulence and competitiveness in *Agrobacterium tumefaciens* C58

Ephraim Aliu *et al.*

Corresponding author: Kan Wang, kanwang@iastate.edu

Sci. Adv. **11**, eadx7408 (2025)
DOI: 10.1126/sciadv.adx7408

This PDF file includes:

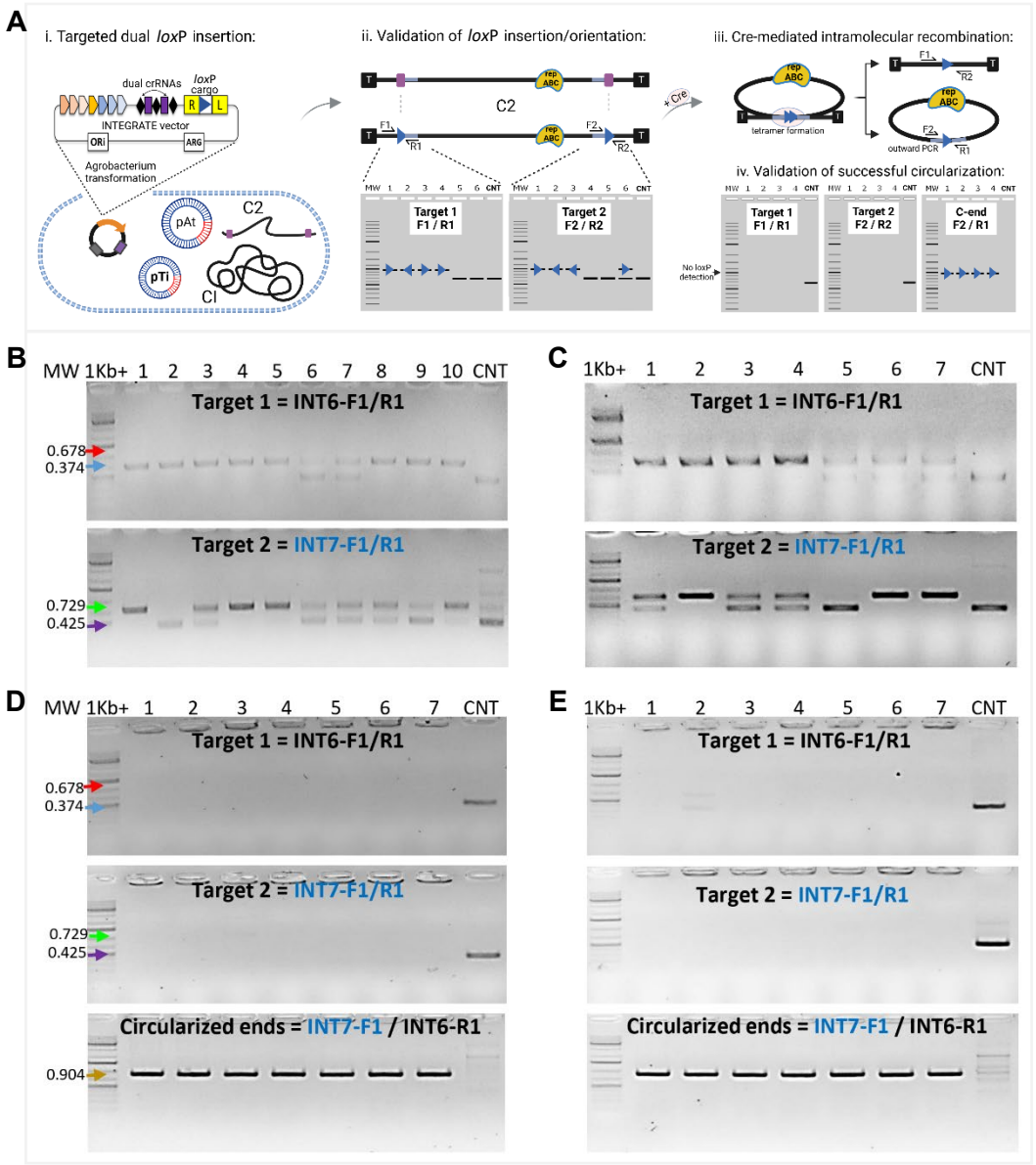

Fig. S1. Circularization of *Agrobacterium* linear replicons. (**A**) Step i: an INTEGRATE vector containing a *lox*P mini-transposon (Tn) cargo with dual crRNAs targeting sub-telomeric regions is introduced into *Agrobacterium*. Step ii: Colony PCR screens to detect successful targeted Tn insertion at the target sites in resulting colonies. Step iii: Colonies with dual *lox*P insertions in the same orientation proceed to Cre-mediated recombination to achieve circularization. After recombination, the original forward (target 1, F1) and reverse (target 2, R2) primer binding sites are no longer detectable. Instead, outward PCR using forward (target 2, F2) and reverse (target 1, F1) primers confirms successful circularization and the presence of a residual *lox*P site. Agarose gel showing dual *lox*P insertion screening in (**B**) WT, wild-type C58 and (**C**) FL, C58F with fused linear chromosome as described. For the first target *lox*P insertion, primers INT6-F1 and INT6-R1 yield a 678 bp band (red arrow) indicating successful *lox*P-cargo Tn insertion, or a 374 bp band (blue arrow) indicating unsuccessful insertion, consistent with the negative control (CNT). For the second *lox*P insertion, primers INT7-F1 and INT7-R1 generate a 729 bp band (green arrow) for successful insertion, and a 425 bp band (purple arrow) for failed insertion. As previous reported (29), mixed insertion mutants were observed in lanes 6 & 7 for WT and lanes 3 & 4 for FL. Outward PCR screening confirmed successful Cre-mediated circularization, resulting in mutants Cir with circularized C2 chromid (**D**) and FCir with a circularized C1-C2 fused chromosome (**E**). Following circularization, colony PCR no longer detects the dual-inserted *lox*P Tn cargo due to the loss of INT6-F1 and INT7-R1 primer binding sites. Outward PCR using primers INT7-F1 and INT6-R1 produces a ~904 bp DNA band representing the circularized chromosome ends, distinct from the negative control. Schematic diagrams were created using Biorender.

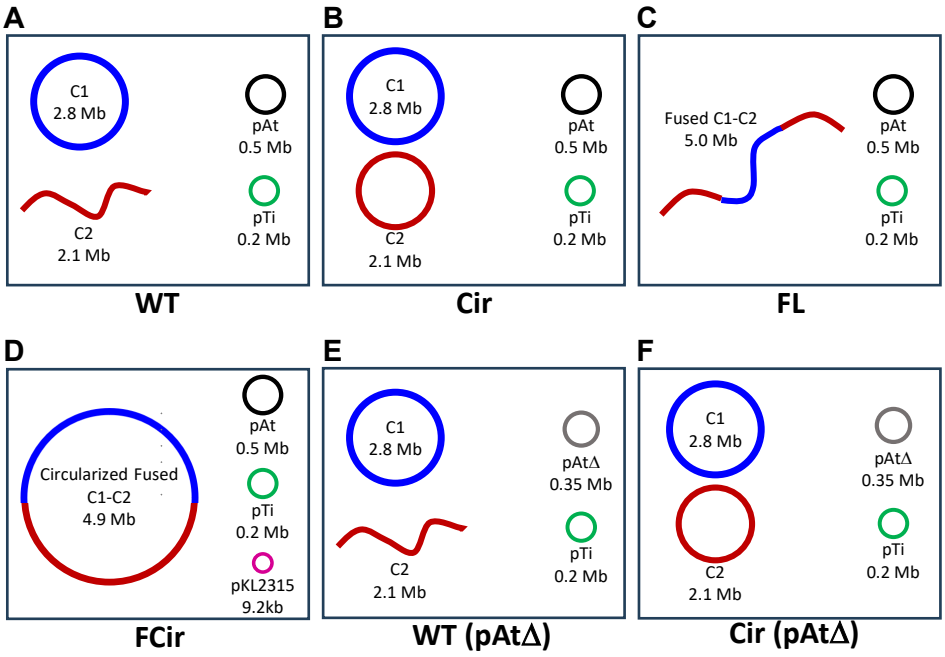

G

	Contig (bp)						
Strains	**C1**	**C2**	**C1-C2 fusion**	**pAT**	**pTi**	**Plasmidsaurus ID**	**References**
WT	2,841,610	2,110,203	NA	542,876	214,242	83B8X8_1	15, 16
Cir	2,841,590	2,075,050	NA	542,872	214,237	83B8X8_2	This study
FL	NA	NA	5,008,288	348,436	214,235	83B8X8_3	Community source, origin unknown
FCir	NA	NA	4,916,611	348,433	214,235	83B8X8_4	This study
WT (pAtΔ)	2,841,591	2,117,599	NA	348,744	214,236	CZQBSL_1	This study
Cir (pAtΔ)	2,841,586	2,075,055	NA	348,709	214,235	CZQBSL_2	This study

NA, not applicable

Fig. S2. Plasmidsaurus™ contig data for C58 variants, with schematic representations redrawn from original Plasmidsaurus™ output. (A) WT, wild-type C58. (**B**) Cir, C58 with circularized C2 chromid. (**C**) FL, C58 with fused C1-C2 replicons. (**D**) FCir, C58 with circularized, fused C1-C2 replicons. The Cre recombinase vector pKL2315 (29) remains resistant to sacB-mediated sucrose curing in FCir post-circularization. (**E**) WT (pATΔ), wild-type C58 harboring a truncated pAT. (F) Cir (pATΔ), circularized C2 strain harboring a truncated pAT. (**G**) Summary of strain contig information obtained from Plasmidsaurus™. All strains retain the wild-type pTi. Strains FL and FCir harbor a pAt replicon with a natural truncation of ~194 kb (30). Strains WT (pATΔ) and Cir (pATΔ) contain a targeted ~194 kb deletion in pAt generated in this study.

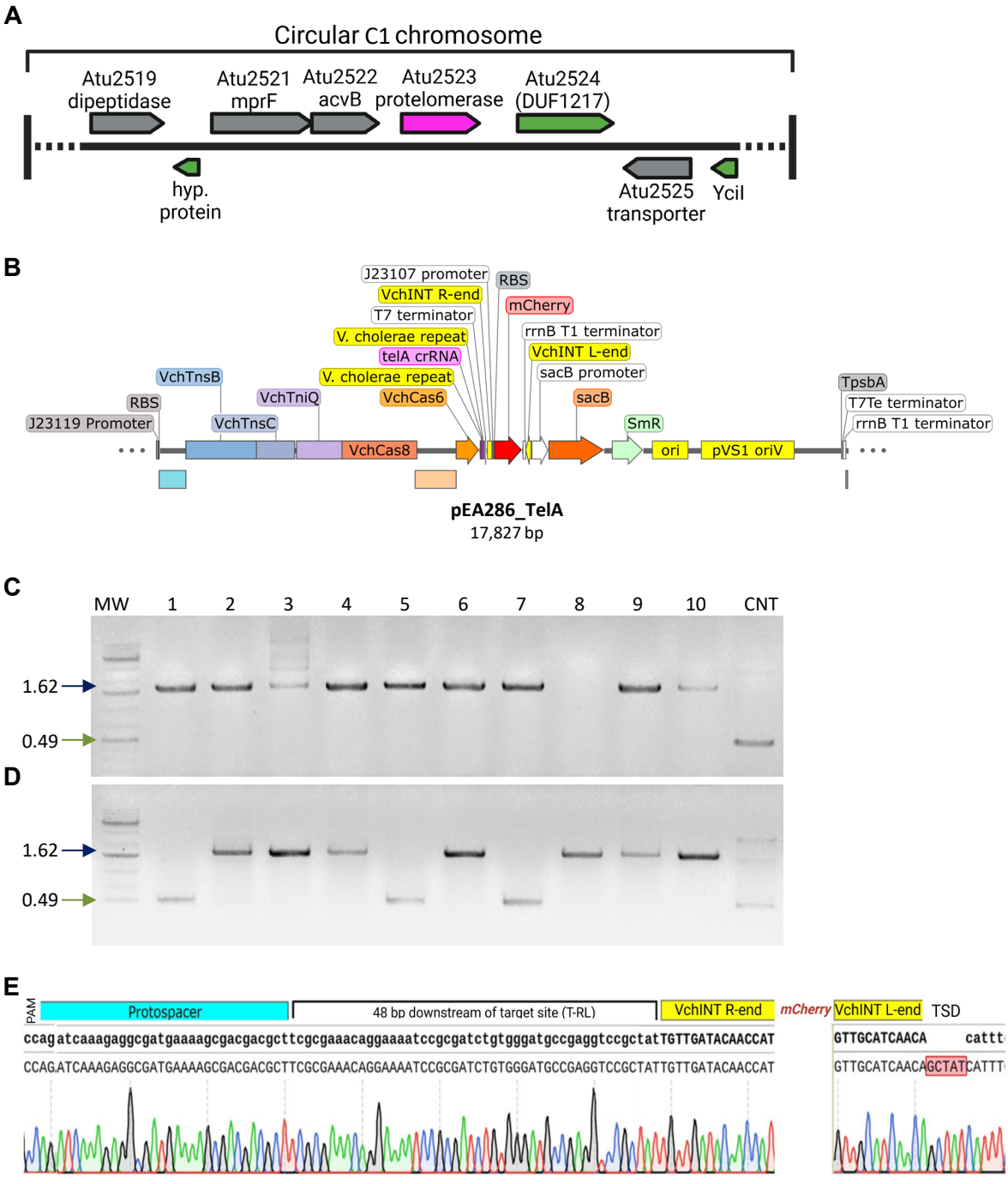

Fig. S3. Knockout of the protelomerase encoded *Atu2523 (telA)* gene in Cir and FCir strains. (**A**) Genomic context of telA and neighboring genes on the primary circular C1 chromosome, based on GenBank accession number NC_003062. Gene orientations are indicated, with dark gray blocks representing genes of known or predicted functions, the purple block indicating the essential protelomerase gene *telA*, and green blocks denoting open reading frames (ORFs) with predicted transposase-related functions. (**B**) Schematic of the INTEGRATE vector pEA286 (see table S1), carrying a *telA*-targeting crRNA (purple) and a J23107-mCherry mini-transposon (Tn) cargo. (**C, D**) Agarose gel electrophoresis confirms successful *telA* mutagenesis in Cir (**C**) and FCir (**D**) strains. A 1.62 kb band (dark blue arrows) in mutant strains indicates successful cargo insertion, whereas a 0.49 kb band (green arrows) from wild-type C58 genomic DNA (CNT) serves as a negative control. Lanes 1 to 10 represent individual screened colonies. (**E**) Sanger sequencing confirmed integration of the mini-Tn cargo DNA into the *telA* locus, 48 bp downstream of the protospacer sequence in both Cir and FCir strains. TSD, target site duplication.

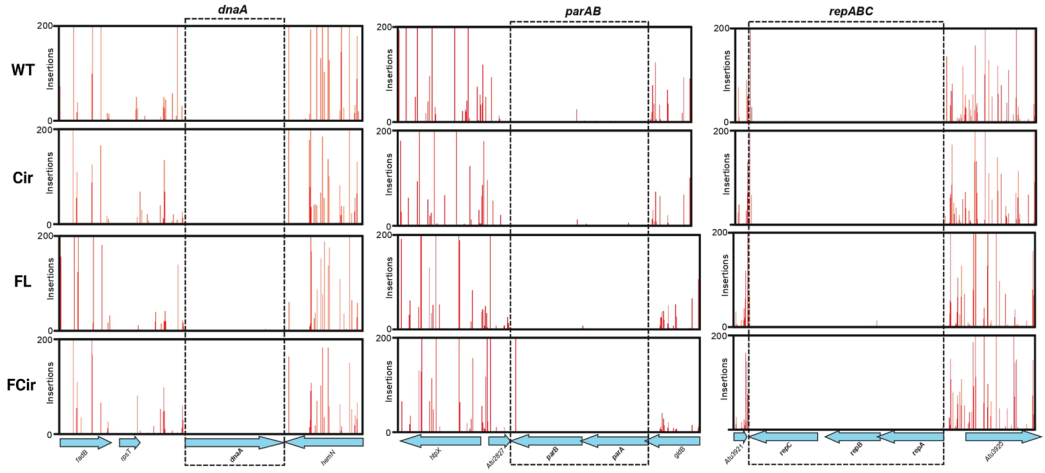

Fig. S4. Tn-seq analysis of replicon origins in C58 variants. Transposon sequencing (Tn-seq) profiles are shown for key replication and partitioning genes in C58 replicons: the *dnaA* gene encoding the C1 replication initiator (left), the *parAB* partitioning system of C1 (middle), and the *repABC* replication and segregation system of C2 (right). The x-axis depicts genome position, and the y-axis represents the number of transposon insertions at each site.

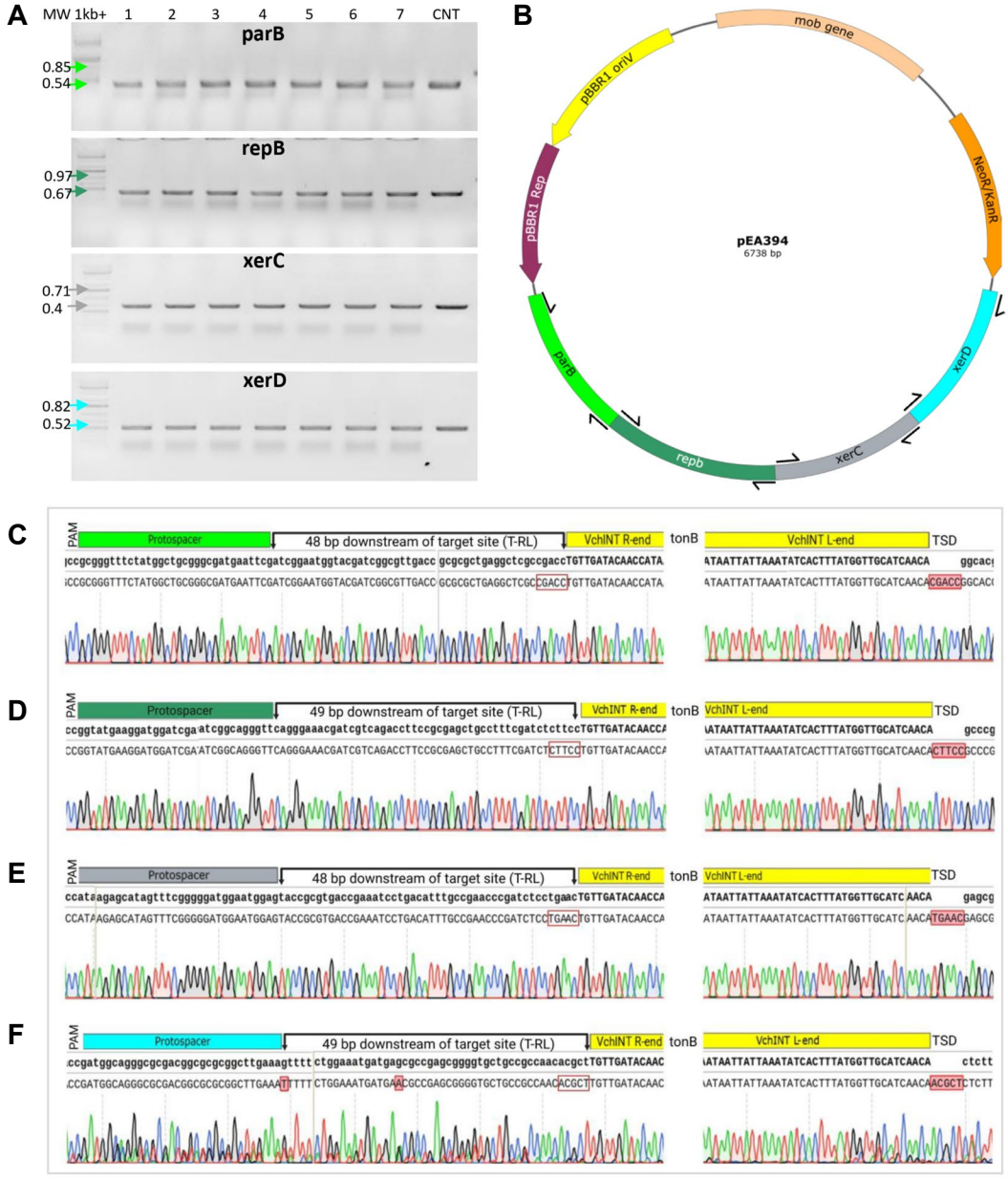

Fig. S5. Requirement of replication and *xerC/D* genes in strain FCir. The *tonB* cargo INTEGRATE vectors – pEA385, pEA386, pEA388, and pEA389 (table S1) – each carrying crRNAs targeting *xerC*, *xerD*, *parB*, and *repB*, respectively, were individually transformed into the FCir strain. (**A**) Agarose gel electrophoresis showed that all target sites resisted insertional mutagenesis, as only the wild-type C58 genomic DNA band (negative control, CNT) was observed. No higher molecular weight bands indicative of Tn insertion were detected. (**B**) To verify crRNA functionality for mutagenesis, partial fragments of each target site, including the crRNA protospacer and primer binding sites, were cloned into the vector pEA394. (**C**–**F**) Sanger sequencing confirmed successful insertion of the *tonB* terminator mini-Tn cargo into the cloned target sites within pEA394: insertion occurred 48 bp downstream of the protospacer for *parB* (**C**) and *xerC* (**E**), and 49 bp downstream of *repB* (**D**) and *xerD* (**F**). In all cases, the transposon was inserted in the T-RL orientation. TSD, target site duplication.

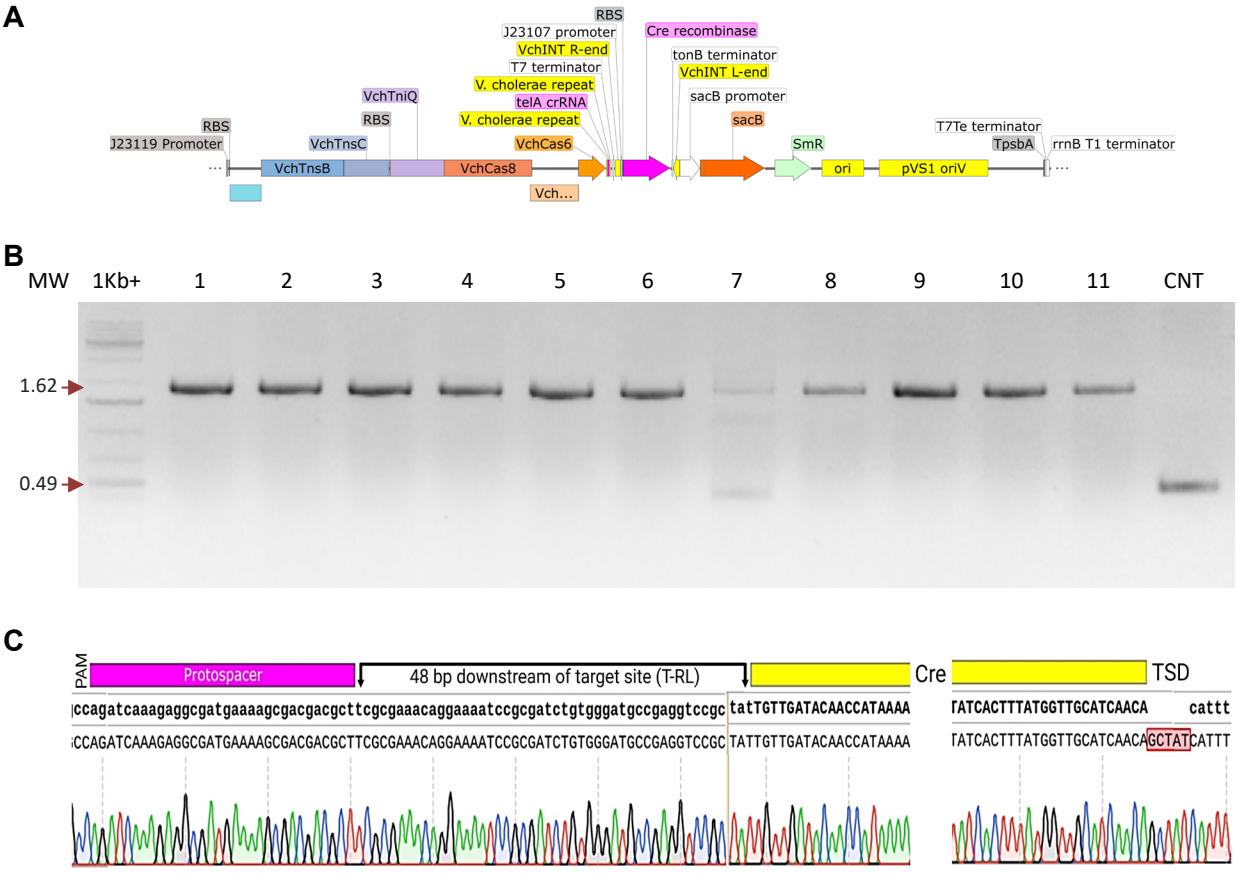

Fig. S6. Generation of the FCir-cre strain. (**A**) Schematic of the INTEGRATE vector pEA393, which carries a crRNA targeting the *telA* gene. The mini-transposon (Tn) cargo includes the *cre* recombinase gene under the control of the constitutive J23107 promoter. (**B**) Agarose gel electrophoresis confirms successful insertion of the Tn cargo into the *telA* target site. All screened colonies displayed a higher molecular weight DNA band (1.62 kb) compared to the wild-type C58 genomic DNA negative control (CNT), which showed a 0.49 kb band, indicating successful Tn cargo insertion. (**C**) Sanger sequencing verified the targeted integration of the cargo DNA into the *telA* locus, 48 bp downstream of the protospacer sequence. The dinucleotide 5’-CC-3’ PAM is shown upstream of the protospacer. TSD, target site duplication.

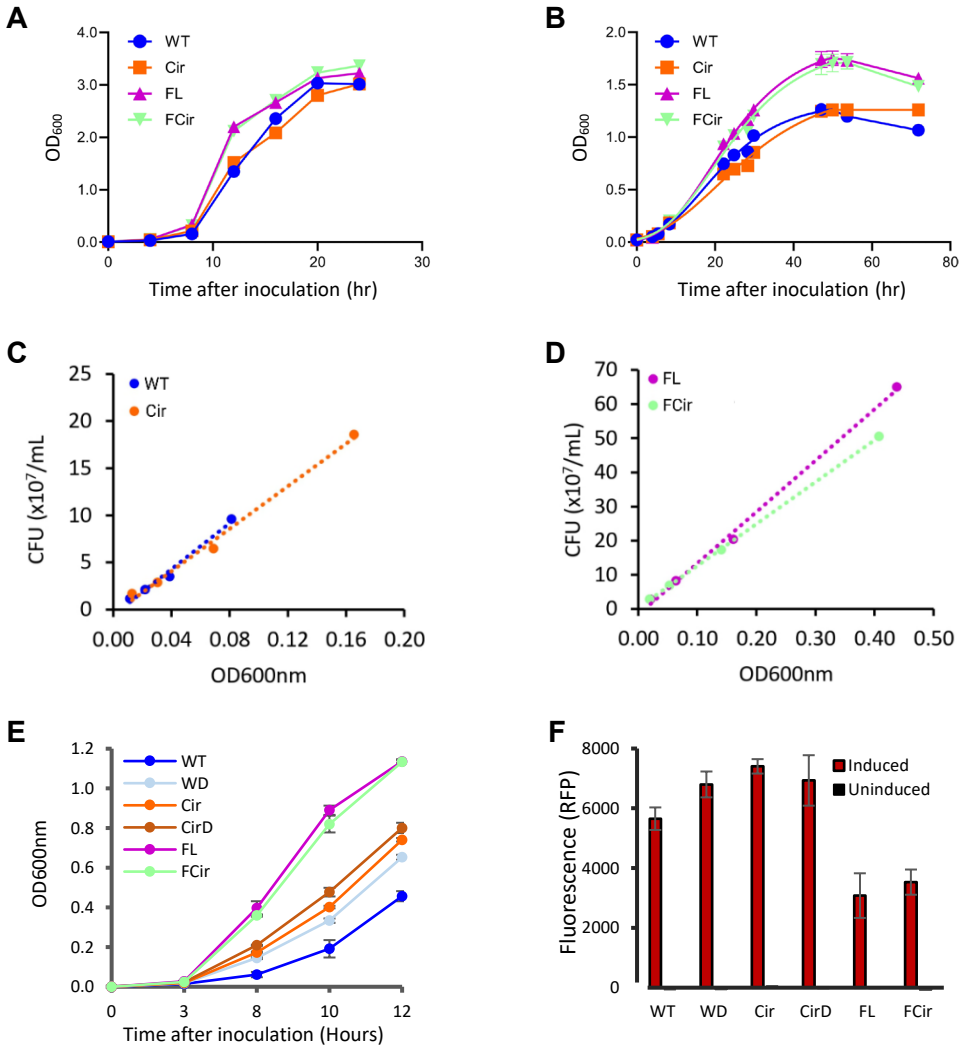

Fig. S7. Growth, cell viability, and virulence evaluation of C58 variants. The optical density at 600 nm (OD_{600}) of *Agrobacterium* cultures was measured over 24 h using a spectrophotometer to monitor growth. (**A**) Growth curves of WT (blue), Cir (orange), FL (purple), and FCir (green) in YEP rich medium. (**B**) Growth curves of the same strains in AB nutrient-limiting medium. (**C, D**) Cell-viability assay of each strain. Colony-forming units (CFU) and OD_{600} were measured every two hours for the first 8 hours of growth in YEP medium. Trendlines show strong correlations between CFU and OD_{600} in (**C**) WT and Cir, and (**D**) FL and FCir. (**E**) Growth curve of all strains, including truncated pAt variants: WT (pATΔ) (WD, light blue) and Cir (pATΔ) (CirD, dark orange). (**F**) Quantification of AS-induced *mCherry* expression driven by the VirG-inducible *virB* promoter. Data represent mean $\pm$ SD from N = 12 biological replicates in (**A**), N = 6 in (**B**), N = 3 in (**C-E**) and are pooled from N = 3 independent biological replicates in (**F**).

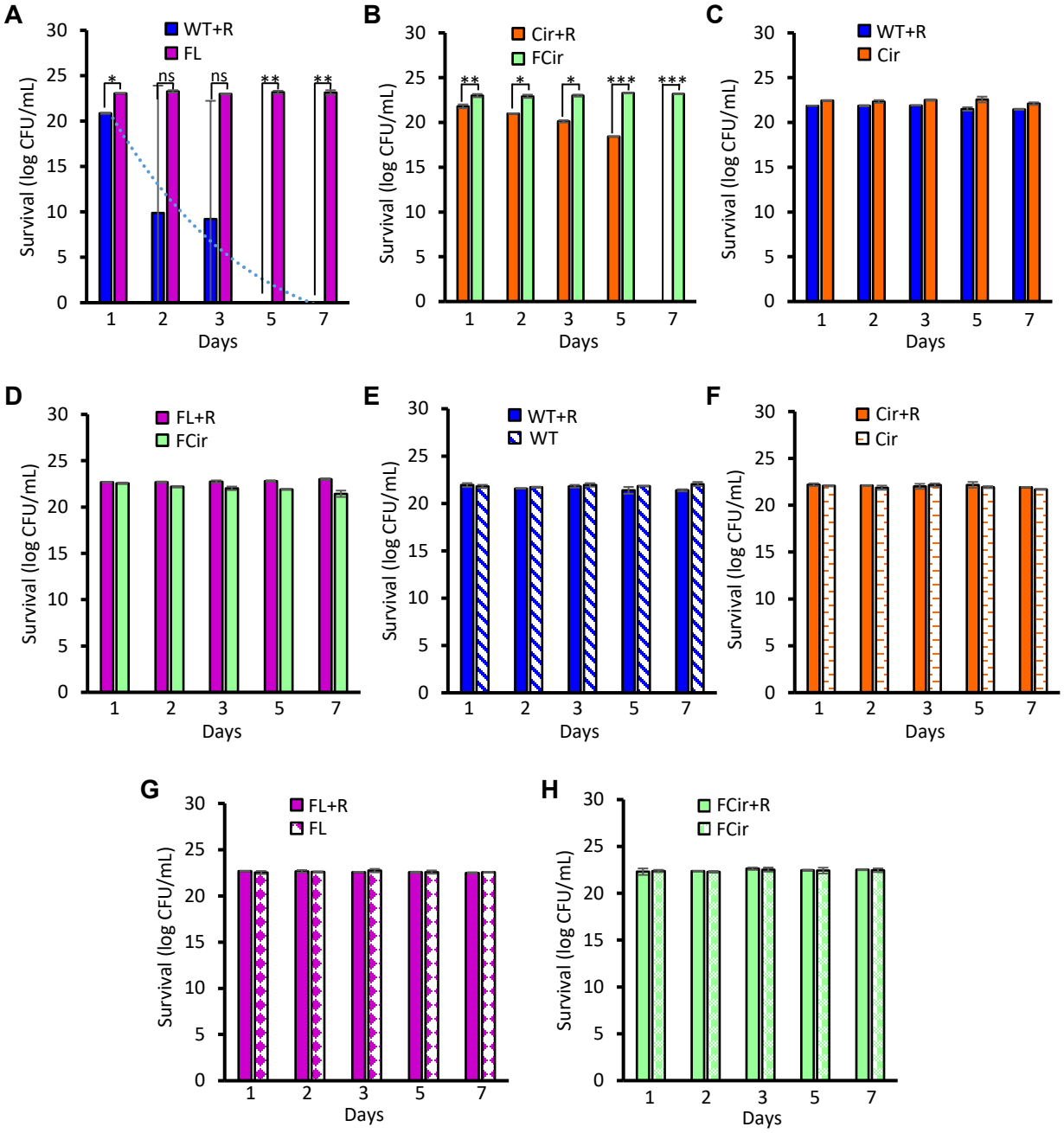

Fig. S8. Reciprocal and self-competition of C58 variants. Relative fitness was assessed through pairwise competition assays between RFP-tagged (+R) strains and their corresponding non-tagged C58 variants. (**A**) WT+R vs FL, (**B**) Cir+R vs FCir, (**C**) WT+R vs Cir, and (**D**) FL+R vs FCir. Self-competition controls: (**E**) WT+R vs WT, (**F**) Cir+R vs Cir, (**G**) FL+R vs FL, and (**H**) FCir+R vs FCir. Statistical significance was determined using a two-sided Student's *t*-test (***, $p < 0.001$, **, $p < 0.01$, *, $p < 0.05$, ns, not significant). Data represent mean ± SD from N = 4 biological replicates.

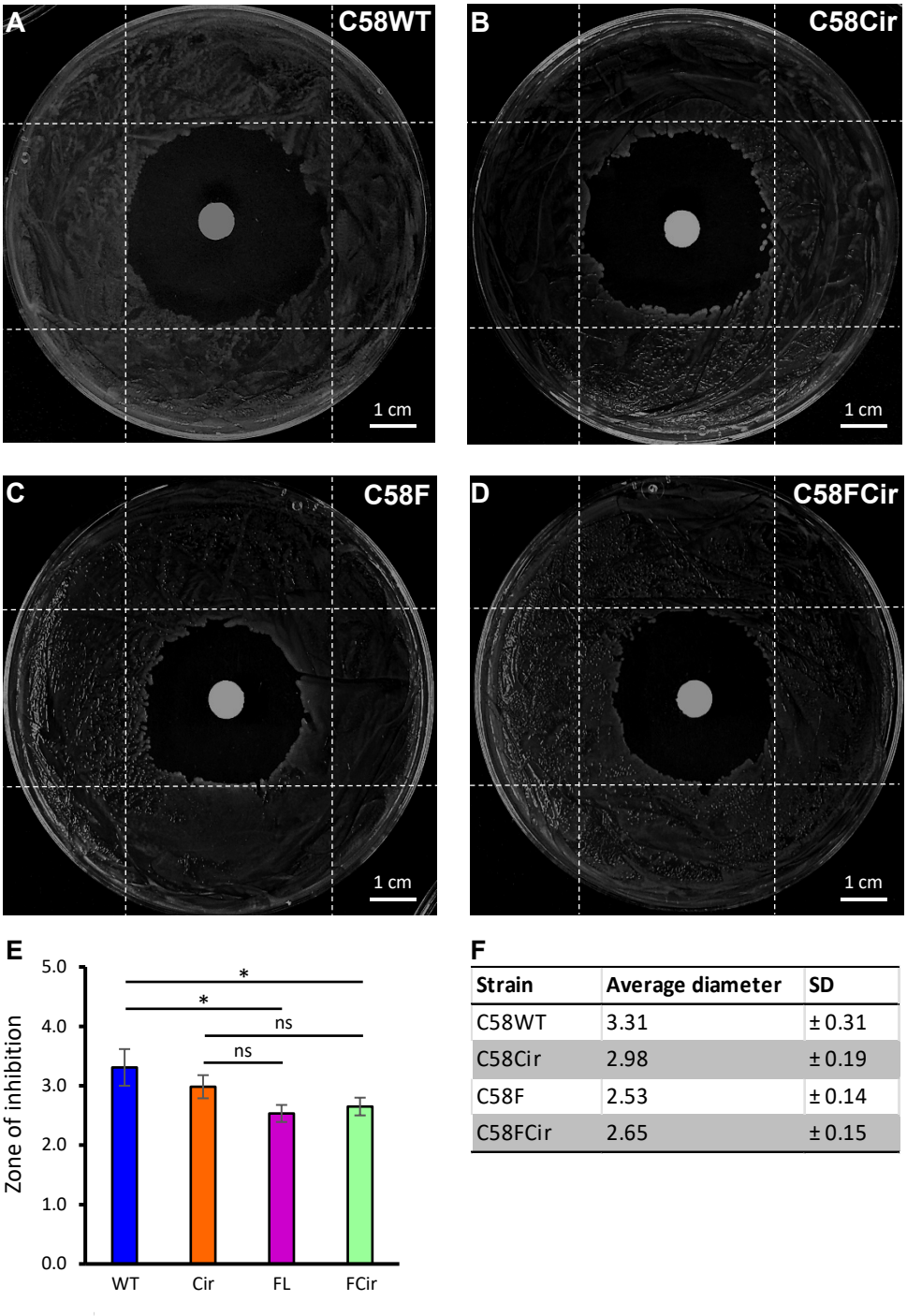

F

Strain	Average diameter	SD
C58WT	3.31	± 0.31
C58Cir	2.98	± 0.19
C58F	2.53	± 0.14
C58FCir	2.65	± 0.15

Fig. S9. Tolerance to peroxide-induced stress in C58 variants. For the H_2O_2 stress assay, a 7 mm filter paper disk was soaked in 30% H_2O_2 for 2 min, air-dried for 6 min, and placed at the center of a YEP agar plate. *Agrobacterium* cells were spread on the YEP plates containing H_2O_2 disk, and zones of growth inhibition were measured two days after incubation for (**A**) WT, (**B**) Cir, (**C**) FL, and (**D**) FCir. (**E**) Quantification of inhibition zone diameters (in cm) displayed as a bar chart. (**F**) Tabulated inhibition zone measurements. Scale bar = 1 cm. Data represent mean ± SD from N = 3 biological replicates.

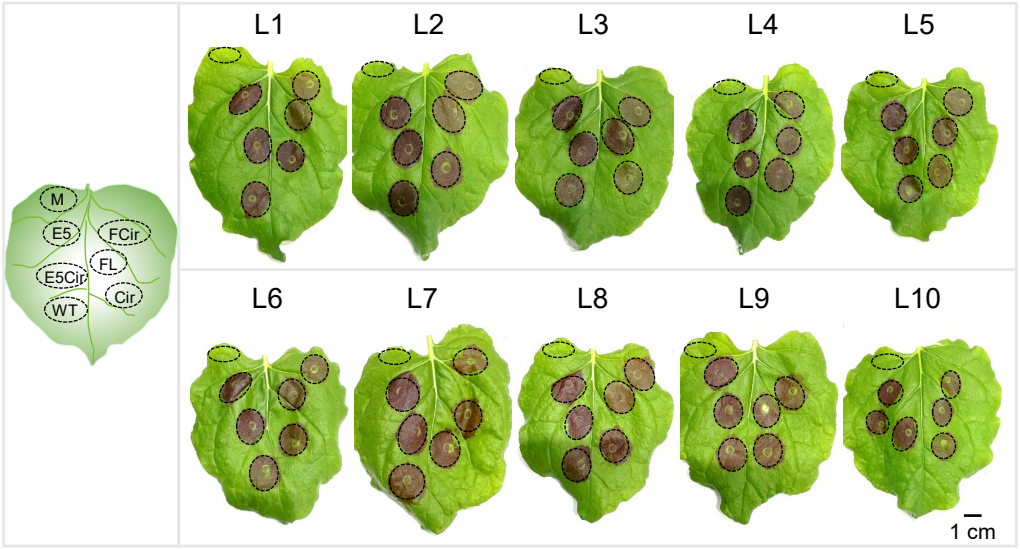

Fig. S10. Transient transformation evaluation via agroinfiltration of *Nicotiana benthamiana* leaves. Each leaf was infiltrated with six *Agrobacterium* strains harboring the binary vector pCBL101-RUBY (93), which carries the RUBY reporter construct. Agroinfiltration was repeated on ten leaves (L1 to L10). Two days post-inoculation, the infiltrated leaf areas were individually collected, and betalain content was quantified as described in Materials and Methods (Evaluation of virulence via RUBY expression assay). The cartoon on the left illustrates the approximate locations of the six infiltration sites per leaf for: EHA105 (or E5), EHA105Cir (or E5Cir), WT, Cir, FL, and FCir. M denotes buffer-only mock inoculation control.

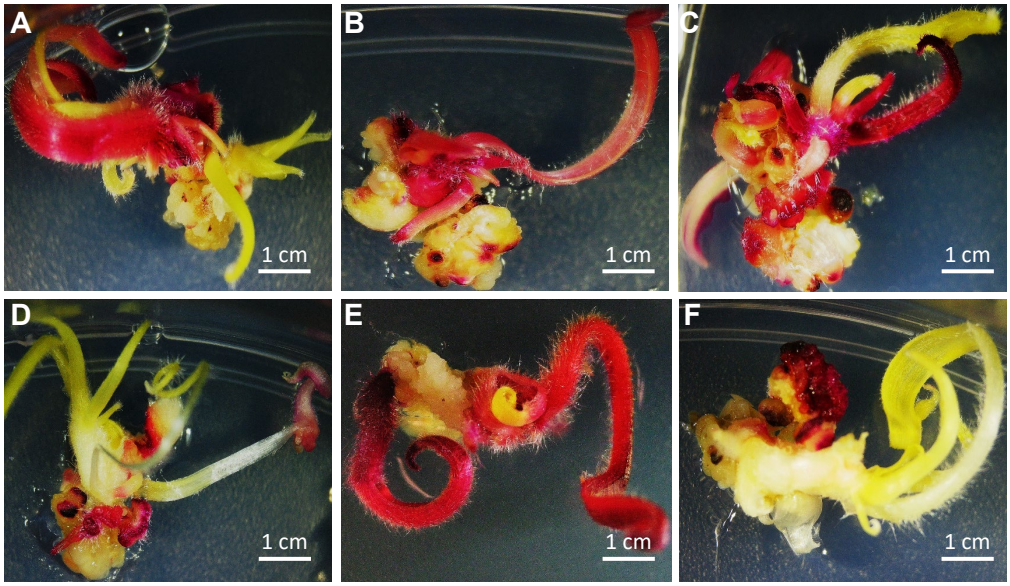

G

ID #	Strain	# embryo infected	Rooted plantlets	Transformation frequency	RUBY +
Exp 1	E5Cir	128	12	9.38%	11
	E5	125	10	8.00%	10
Exp 2	E5Cir	126	6	4.76%	5
	E5	130	4	3.08%	3

Fig. S11. Comparison of E5 and E5Cir strains in stable maize B104 transformation. Regenerating maize B104 shoots expressing the *RUBY* reporter gene, imaged 4 weeks post-infection. Shoots from *Agrobacterium* infection using strain E5Cir (**A – C**) and wild-type E5 (**D – F**). (**G**) Summary of transformation frequencies of two independent infection experiments. E5, EHA105; E5Cir, EHA105Cir. Both strains carry a binary vector pCB101-RUBY and a ternary *vir* helper plasmid pKL2299A (93).

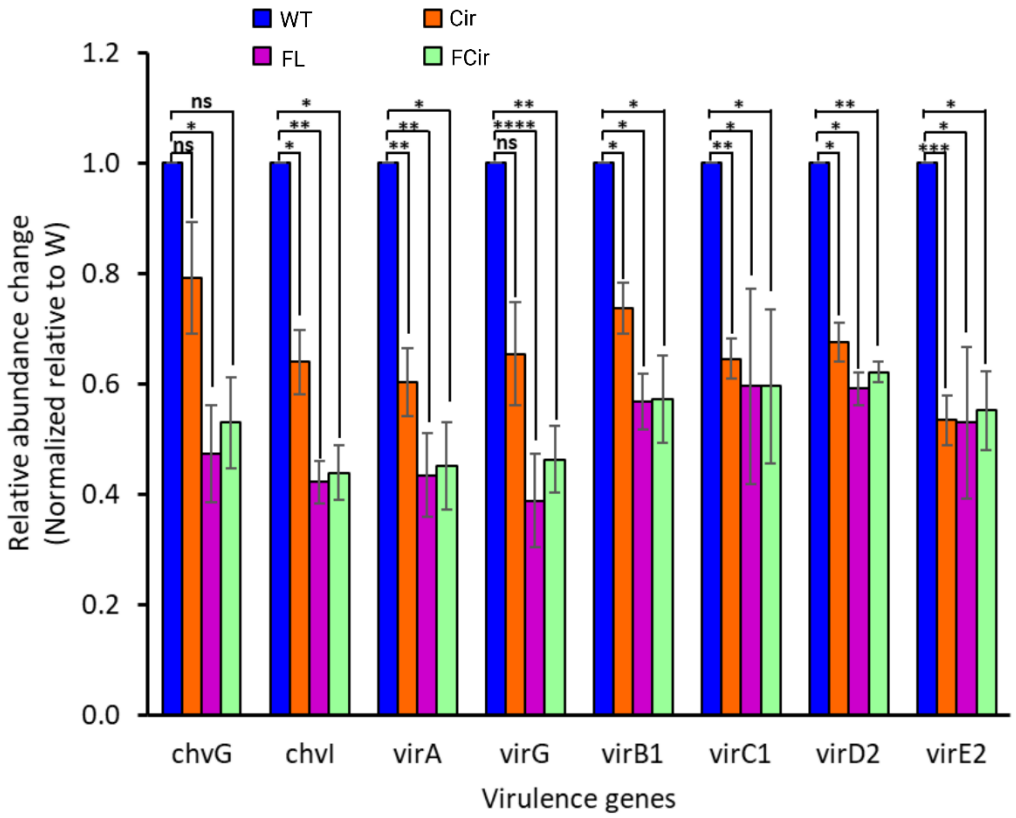

Fig. S12. RT-qPCR analysis of *vir* gene expression in C58 variants. Expression levels of selected *vir* genes were measured in *Agrobacterium* C58 variants. Transcript levels were normalized to the housekeeping gene *rpoD* (encoding the RNA polymerase sigma factor) as a control. Relative gene expression was calculated using the $2^{-\Delta\Delta Ct}$ method (76) and normalized to expression levels in the wild-type C58 strain (see Materials and Methods). Error bars represent standard deviations of the mean from $N = 3$ biological replicates. Statistical significance was assessed using a two-tailed paired sample *t*-test (****, $p < 0.0001$; ***, $p < 0.001$; **, $p \leq 0.01$; *, $p \leq 0.05$; ns, not significant).

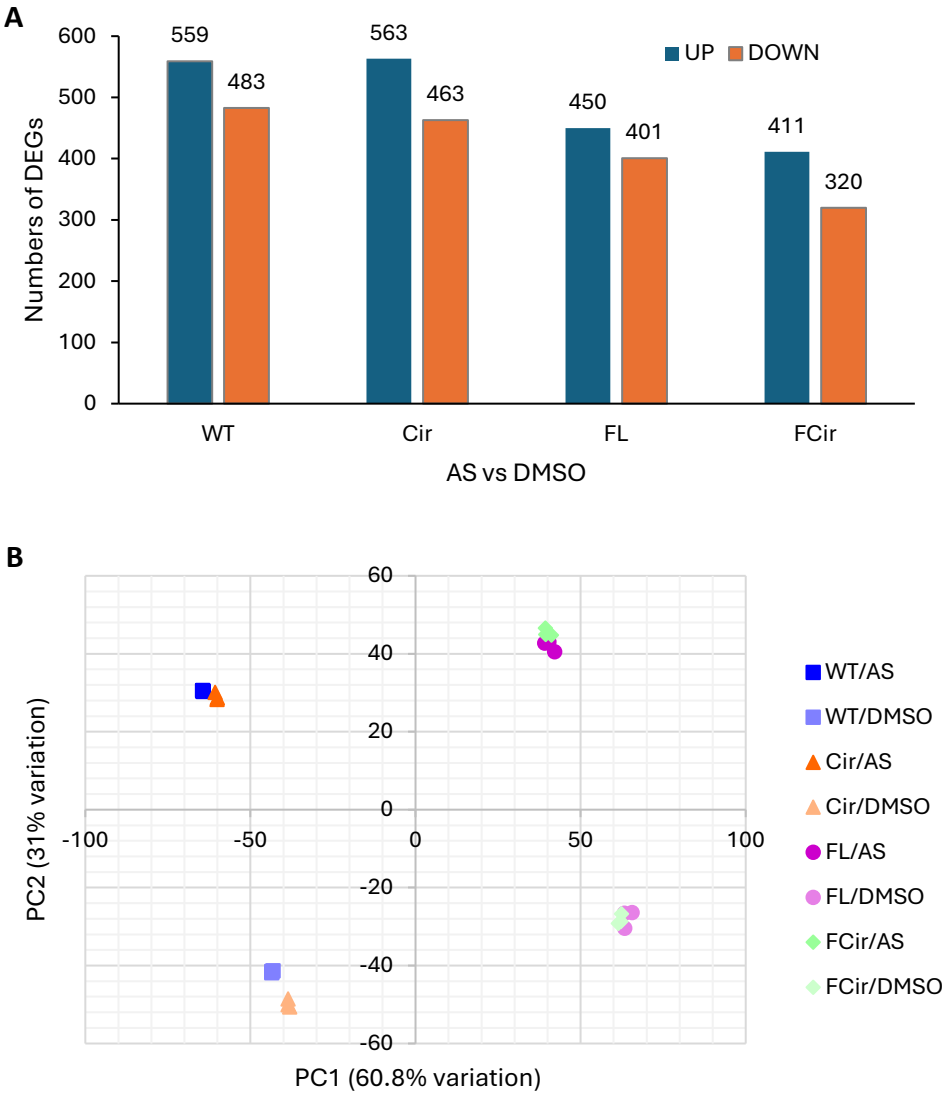

Fig. S13. Summary of transcriptomes for C58 variants under AS-induced and non-induced conditions. (**A**) Number of differentially expressed genes (DEG; ≥2 fold-change, $p < 0.05$) in response to acetosyringone (AS) treatment compared to DMSO control. (**B**) Principal Component Analysis (PCA) plot showing transcriptomic variation among all samples. Strain abbreviations: WT, wildtype C58; Cir, C58 with circularized C2 chromid; FL, C58 with fused C1-C2 linear chromosome; FCir, C58 with circularized fused C1-C2 chromosome. RNA-seq was performed with *N* = 3 biological replicates per condition.

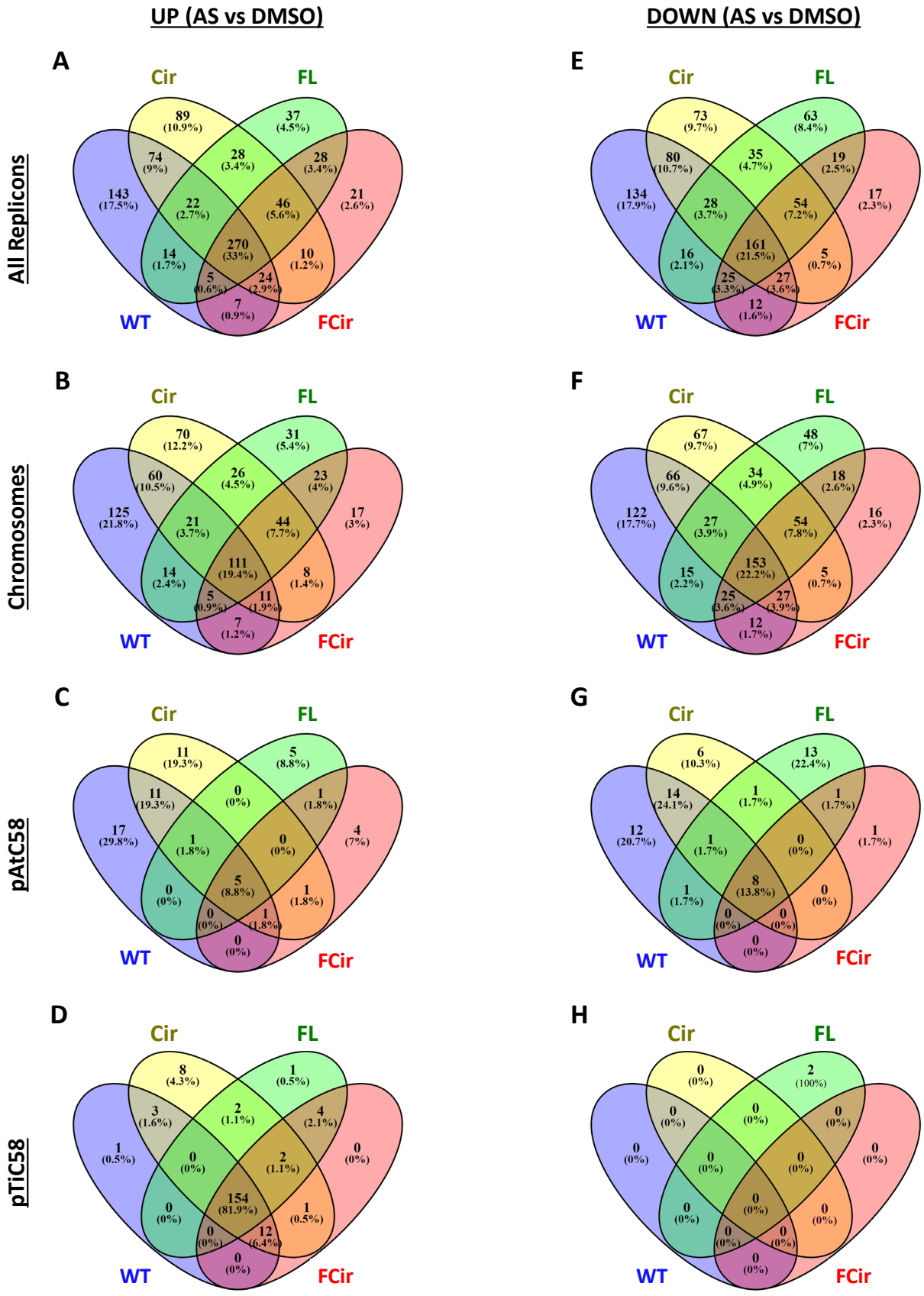

Fig. S14. Venn diagrams of UP- and DOWN-regulated DEGs across C58 variants and replicons. (**A-D**) Up-regulated differentially expressed genes (DEGs). (**E-H**) Down-regulated DEGs. Each Venn diagram illustrates the overlap of DEGs among C58 variants. Percentages in each segment indicate the proportion of genes relative to the total number of up-regulated (**A-D**) or down-regulated (**E-H**) DEGs within: (**A, E**) all replicons; (**B, F**) chromosomes C1 and C2; (**C, G**) plasmid pAtC58; (**D, H**) plasmid pTiC58. Strain abbreviations: WT, wildtype C58; Cir, C58 with circularized C2 chromid; FL, C58 with fused C1-C2 linear chromosome; FCir, C58 with circularized fused C1-C2 chromosome.

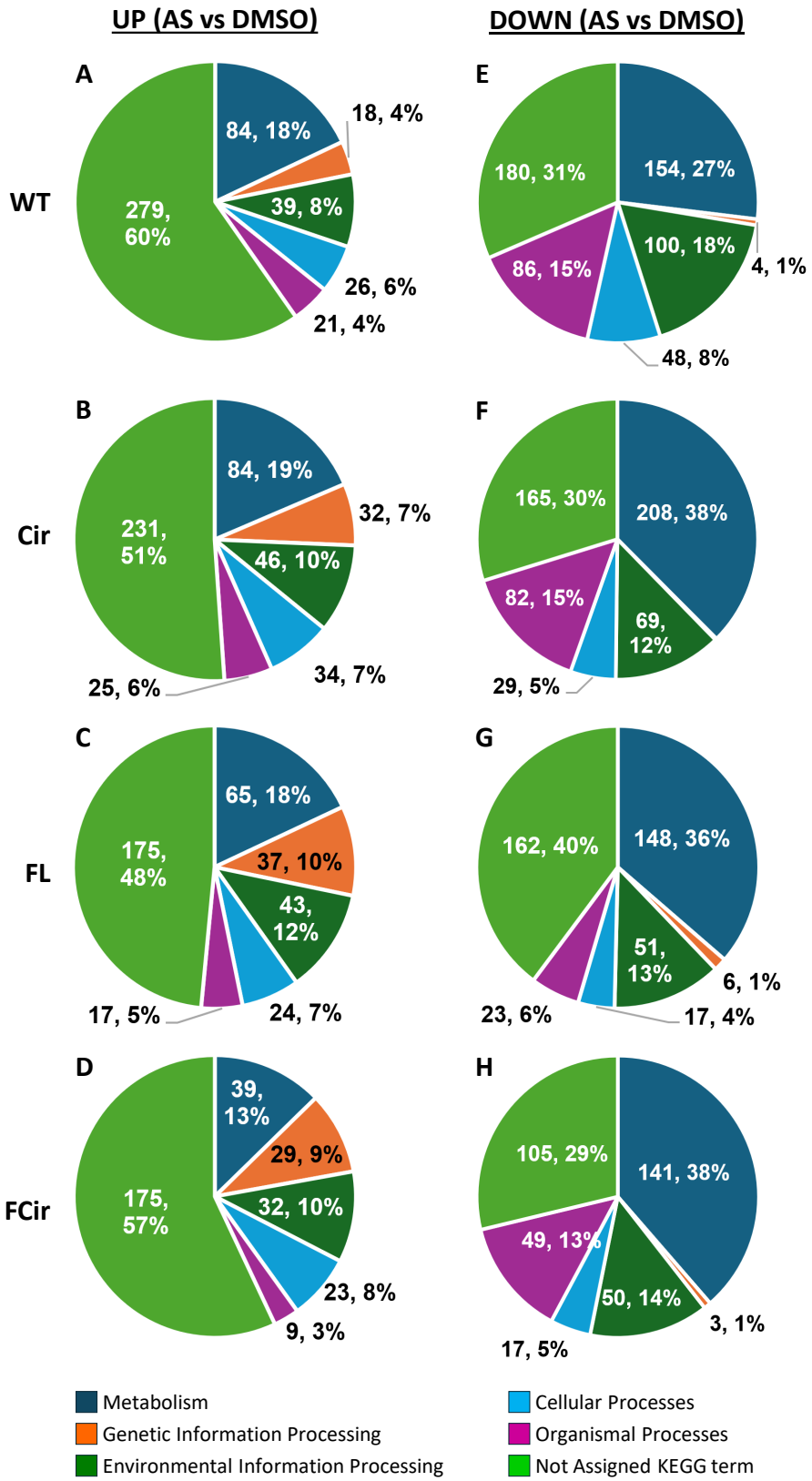

Fig. S15. KEGG pathways distribution of differentially expressed genes in C58 variants under acetosyringone induction. (**A-D**) KEGG categories of upregulated genes. (**E-H**) KEGG categories of downregulated genes. Each panel shows the number and proportion of DEGs assigned to Kyoto Encyclopedia of Genes and Genomes (KEGG) pathways under acetosyringone (AS) treatment. Values represent both gene counts and percentages within each KEGG category. Gene IDs and corresponding KEGG terms are listed in table S3. Strain abbreviations: WT, wildtype C58; Cir, C58 with circularized C2 chromid; FL, C58 with fused C1-C2 linear chromosome; FCir, C58 with circularized fused C1-C2 chromosome. Additional data tables are provided in table S3.

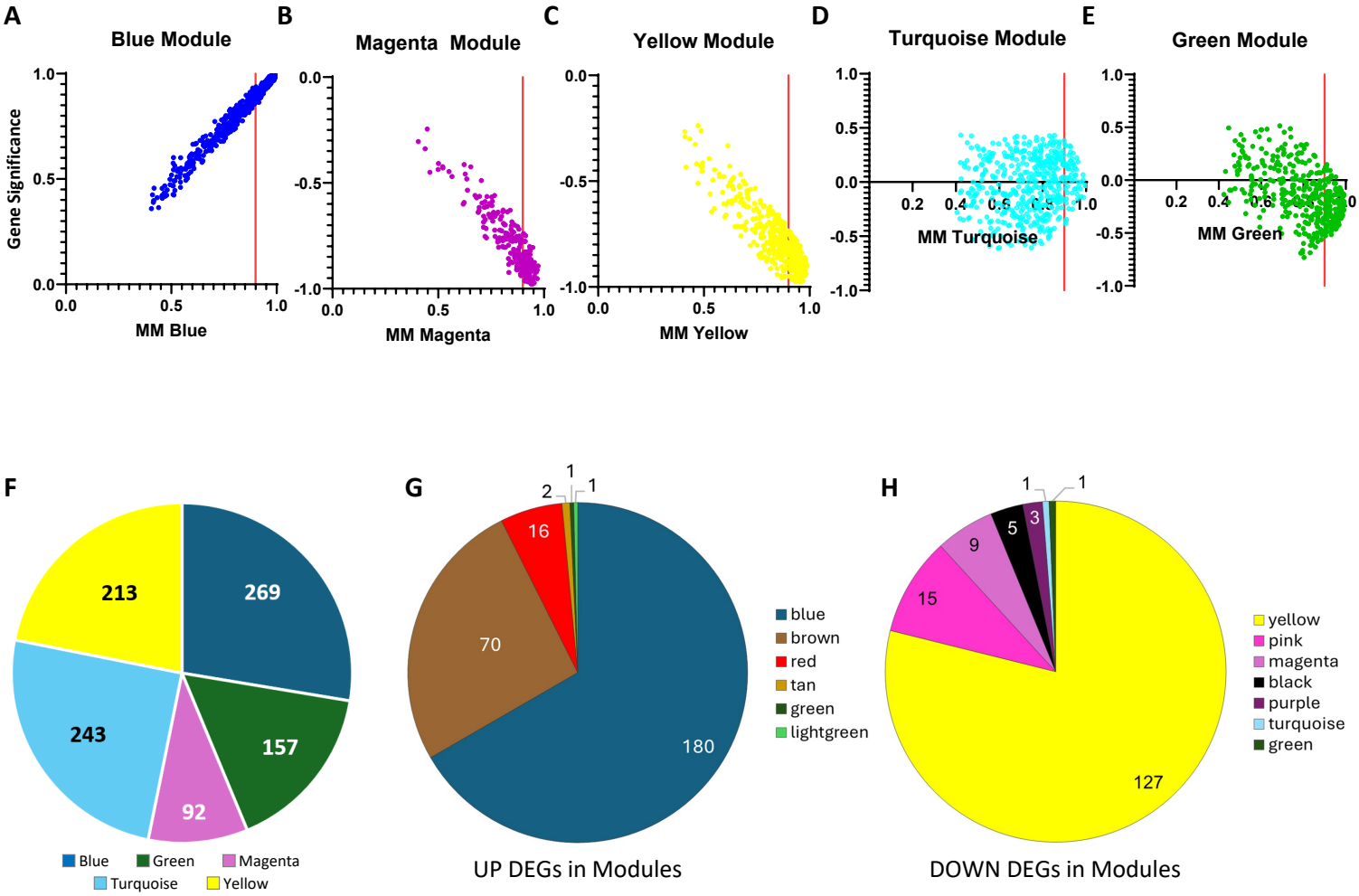

Fig. S16. WGCNA: Relationship of genes in modules of interest and acetosyringone conditions. (**A-E**) Scatterplots showing gene significance for the acetosyringone (AS) condition vs module membership (MM) for five selected co-expression modules. Vertical lines indicate the MM threshold (MM = 0.9), highlighting strongly connected (hub) genes within each module. (**F**) Number of genes with MM > 0.9 in each selected module. (**G, H**) Assignment of differentially expressed genes (DEGs) to WGCNA modules. (**G**) Number of upregulated (UP) and (H) number of downregulated (DOWN) genes assigned to each module. Modules were selected based on their correlation with AS treatment. DEGs were identified as genes showing ≥2-fold change in expression with $p < 0.05$. Additional data tables are provided in table S3.

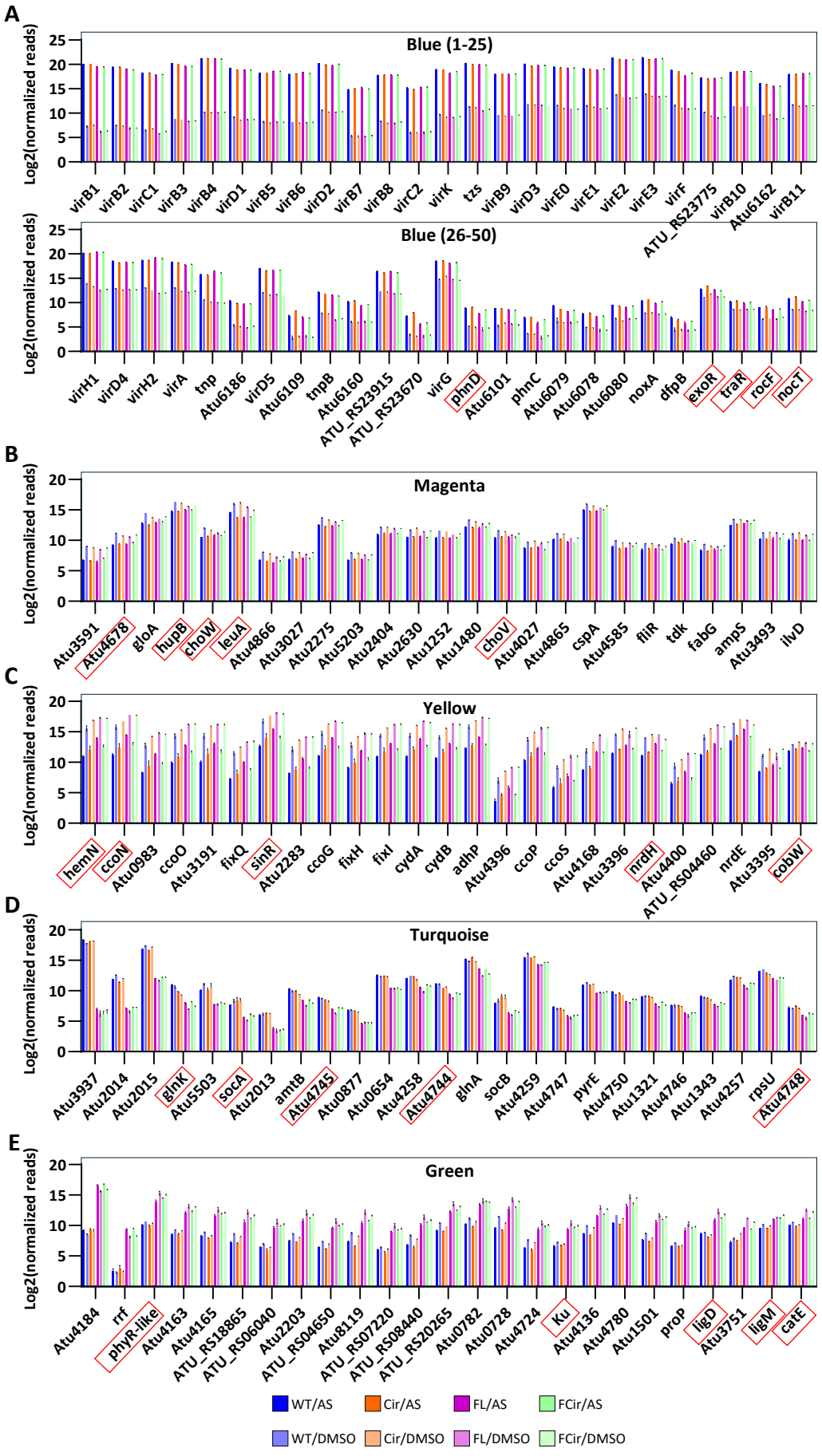

Fig. S17. Expression profiles of representative genes with module membership >0.9 from each WGCNA module. (**A**) Blue, (**B**) Magenta, (**C**) Yellow, (**D**) Turquoise, and (**E**) Green modules. Genes in (**A-C**) are ordered by fold change between acetosyringone (AS) and DMSO conditions (from greatest to lowest). Genes in (**D, E**) are ordered by the expression difference between WT and FL strains (from greatest to lowest). Genes discussed in the main text are highlighted with a red square. Strain abbreviations: WT, wildtype C58; Cir, C58 with circularized C2 chromid; FL, C58 with fused C1-C2 linear chromosome; FCir, C58 with circularized fused C1-C2 chromosome. Gene names and functional descriptions are provided on the following page.

Blue Module (1-25)

NCBI ID	GenBank ID	Gene Name	Description
ATU_RS23790	Atu6167	virB1	type IV secretion system lytic transglycosylase VirB1
ATU_RS23795	Atu6168	virB2	pilin major subunit VirB2
ATU_RS23855	Atu6180	virC1	conjugal transfer ATPase VirC1
ATU_RS23800	Atu6169	virB3	type IV secretion system protein VirB3
ATU_RS23805	Atu6170	virB4	type IV secretion/conjugal transfer ATPase VirB4
ATU_RS23860	Atu6181	virD1	T-DNA border endonuclease subunit VirD1
ATU_RS23810	Atu6171	virB5	pilin minor subunit VirB5
ATU_RS23815	Atu6172	virB6	type IV secretion system protein
ATU_RS23865	Atu6182	virD2	T-DNA border endonuclease VirD2
ATU_RS23820	Atu6173	virB7	type IV secretion system lipoprotein VirB7
ATU_RS23825	Atu6174	virB8	type IV secretion system protein VirB8
ATU_RS23850	Atu6179	virC2	conjugal transfer protein VirC2
ATU_RS23755	Atu6156	virK	VirK family protein
ATU_RS23780	Atu6164	tzs	(dimethylallyl)adenosine tRNA methylthiotransferase
ATU_RS23830	Atu6175	virB9	P-type conjugative transfer protein VirB9
ATU_RS23870	Atu6183	virD3	protein virD3
ATU_RS23890	Atu6188	virE0	type IV secretion system virulence effector VirE3
ATU_RS23895	Atu6189	virE1	type IV secretion system effector chaperone VirE1
ATU_RS23900	Atu6190	virE2	type IV secretion system single-stranded DNA binding effector VirE2
ATU_RS23905	Atu6191	virE3	virA/G regulated protein
ATU_RS23750	Atu6154	virF	hypothetical protein
ATU_RS23775			hypothetical protein
ATU_RS23835	Atu6176	virB10	type IV secretion system protein VirB10
ATU_RS23770	Atu6162		hypothetical protein
ATU_RS23840	Atu6177	virB11	P-type DNA transfer ATPase VirB11

Blue Module (26-50)

NCBI ID	GenBank ID	Gene Name	Description
ATU_RS23735	Atu6150	virH1	cytochrome P450
ATU_RS23875	Atu6184	virD4	type IV secretion system ATPase VirD4
ATU_RS23740	Atu6151	virH2	cytochrome P450
ATU_RS23785	Atu6166	virA	two-component system sensor kinase VirA
ATU_RS23745		tnp	pseudo
ATU_RS23885	Atu6186		virA/G regulated protein
ATU_RS23880	Atu6185	virD5	virA/G regulated protein
ATU_RS23530	Atu6109		hypothetical protein
ATU_RS26765		tnpB	pseudo
ATU_RS23765	Atu6160		pseudo
ATU_RS23915			IS66 family insertion sequence element accessory protein TnpB
ATU_RS23670			hypothetical protein
ATU_RS23845	Atu6178	virG	two-component system response regulator VirG
ATU_RS00825	Atu0173	phnD	phosphonate ABC transporter substrate-binding protein
ATU_RS23500	Atu6101		lactate dehydrogenase
ATU_RS00830	Atu0174	phnC	phosphonate ABC transporter ATP-binding protein
ATU_RS23395	Atu6079		NtaA/DmoA family FMN-dependent monooxygenase
ATU_RS23390	Atu6078		LLM class flavin-dependent oxidoreductase
ATU_RS23400	Atu6080		LysR family transcriptional regulator
ATU_RS23095	Atu6019	noxA	NAD(P)/FAD-dependent oxidoreductase
ATU_RS23380	Atu6076	dfpB	ABC transporter permease
ATU_RS08400	Atu1715	exoR	exopolysaccharide production regulator ExoR
ATU_RS23655	Atu6134	traR	transcriptional regulator TraR
ATU_RS23090	Atu6018	rocF	arginase
ATU_RS23135	Atu6027	nocT	nopaline ABC transporter substrate-binding protein NocT

Magenta Module

NCBI ID	GenBank ID	Gene Name	Description
ATU_RS16660	Atu3591		SDR family oxidoreductase
ATU_RS21935	Atu4678		transporter substrate-binding domain-containing protein
ATU_RS08825	Atu1802	gloA	VOC family protein
ATU_RS06225	Atu1262	hupB	DNA-binding protein HupB
ATU_RS11125	Atu2280	choW	choline ABC transporter permease subunit
ATU_RS11045	Atu2264	leuA	2-isopropylmalate synthase
ATU_RS22860	Atu4866		pseudo
ATU_RS13925	Atu3027		hydroxyacid dehydrogenase
ATU_RS11100	Atu2275		glyoxalase superfamily protein
ATU_RS24885	Atu5203		MBL fold metallo-hydrolase
ATU_RS11715	Atu2404		GFA family protein
ATU_RS12800	Atu2630		DUF2867 domain-containing protein
ATU_RS06180	Atu1252		hypothetical protein
ATU_RS07290	Atu1480		peroxiredoxin
ATU_RS11120	Atu2279	choV	choline ABC transporter ATP-binding protein
ATU_RS18810	Atu4027		cytochrome c family protein
ATU_RS22855	Atu4865		SDR family oxidoreductase
ATU_RS19695	Atu4214	cspA	cold-shock protein
ATU_RS21505	Atu4585		dihydrofolate reductase family protein
ATU_RS02865	Atu0582	fliR	flagellar biosynthetic protein FliR
ATU_RS11135	Atu2282	tdk	thymidine kinase
ATU_RS25975	Atu5438	fabG	SDR family NAD(P)-dependent oxidoreductase
ATU_RS01315	Atu0274	ampS	aminopeptidase
ATU_RS16180	Atu3493		alpha/beta fold hydrolase
ATU_RS13315	Atu2736	ilvD	IlvD/Edd family dehydratase

Yellow Module

NCBI ID	GenBank ID	Gene Name	Description
ATU_RS07860	Atu1601	hemN	oxygen-independent coproporphyrinogen III oxidase
ATU_RS07590	Atu1537	ccoN	cytochrome-c oxidase, cbb3-type subunit I
ATU_RS04880	Atu0983		carboxymuconolactone decarboxylase family protein
ATU_RS07585	Atu1536	ccoO	cytochrome-c oxidase, cbb3-type subunit II
ATU_RS14730	Atu3191		OmpW family protein
ATU_RS07580	Atu1535	fixQ	
ATU_RS11665	Atu2394	sinR	Crp/Fnr family transcriptional regulator
ATU_RS11140	Atu2283		pseudoazurin
ATU_RS07555	Atu1530	ccoG	cytochrome c oxidase accessory protein CcoG
ATU_RS07550	Atu1529	fixH	FixH family protein
ATU_RS07545	Atu1528	fixI	cation-translocating P-type ATPase
ATU_RS19110	Atu4091	cydA	cytochrome ubiquinol oxidase subunit I
ATU_RS19115	Atu4092	cydB	cytochrome d ubiquinol oxidase subunit II
ATU_RS03065	Atu0626	adhP	alcohol dehydrogenase AdhP
ATU_RS20605	Atu4396		SCP2 domain-containing protein
ATU_RS07575	Atu1534	ccoP	cytochrome-c oxidase, cbb3-type subunit III
ATU_RS07540	Atu1527	ccoS	
ATU_RS19480	Atu4168		YqjD family protein
ATU_RS15715	Atu3396		ABC transporter substrate-binding protein
ATU_RS00325	Atu0068	nrdH	glutaredoxin-like protein NrdH
ATU_RS20625	Atu4400		TonB-dependent receptor
ATU_RS04460			TraR/DksA C4-type zinc finger protein
ATU_RS00335	Atu0070	nrdE	class 1b ribonucleoside-diphosphate reductase subunit alpha
ATU_RS15710	Atu3395		iron ABC transporter permease
ATU_RS13660	Atu2805	cobW	cobalamin biosynthesis protein CobW

Turquoise Module

NCBI ID	GenBank ID	Gene Name	Description
ATU_RS18350	Atu3937		16S ribosomal RNA
ATU_RS09835	Atu2014		ABC transporter substrate-binding protein
ATU_RS09840	Atu2015		PLP-dependent aminotransferase family protein
ATU_RS13415	Atu2757	glnK	P-II family nitrogen regulator
ATU_RS26285	Atu5503		hypothetical protein
ATU_RS23980	Atu5006	socA	ABC transporter substrate-binding protein
ATU_RS09830	Atu2013		iron ABC transporter permease
ATU_RS13420	Atu2758	amtB	ammonium transporter
ATU_RS22265	Atu4745		sugar ABC transporter ATP-binding protein
ATU_RS04320	Atu0877		metallophosphoesterase
ATU_RS03210	Atu0654		LysR substrate-binding domain-containing protein
ATU_RS19915	Atu4258		oligopeptide ABC transporter permease OppB
ATU_RS22260	Atu4744		substrate-binding domain-containing protein
ATU_RS11775	Atu2416	glnA	glutamine synthetase beta-grasp domain-containing protein
ATU_RS26955	Atu5005	socB	amino acid ABC transporter permease/ATP-binding protein
ATU_RS19920	Atu4259		peptide ABC transporter substrate-binding protein
ATU_RS22275	Atu4747		ABC transporter permease
ATU_RS01925	Atu0400	pyrE	orotate phosphoribosyltransferase
ATU_RS22290	Atu4750		sugar phosphate isomerase/epimerase family protein
ATU_RS06515	Atu1321		YjhX family toxin
ATU_RS22270	Atu4746		ABC transporter permease
ATU_RS06625	Atu1343		cysteine hydrolase family protein
ATU_RS19910	Atu4257		ABC transporter permease
ATU_RS16890	Atu3637	rpsU	30S ribosomal protein S21
ATU_RS22280	Atu4748		sugar phosphate isomerase/epimerase

Green Module

NCBI ID	GenBank ID	Gene Name	Description
ATU_RS19555	Atu4184		23S ribosomal RNA
ATU_RS19560	Atu4186	rrf	5S ribosomal RNA
ATU_RS19450	Atu4162	phyR-like	response regulator
ATU_RS19455	Atu4163		sensor histidine kinase
ATU_RS19465	Atu4165		PRC-barrel domain-containing protein
ATU_RS18865			hypothetical protein
ATU_RS06040			hypothetical protein
ATU_RS10755	Atu2203		DUF1236 domain-containing protein
ATU_RS04650			hypothetical protein
ATU_RS01980	Atu8119		PRC-barrel domain-containing protein
ATU_RS07220			DUF3008 family protein
ATU_RS08440			DUF3309 family protein
ATU_RS20265			PRC-barrel domain-containing protein
ATU_RS03860	Atu0782	csbD	CsbD family protein
ATU_RS03590	Atu0728		BA14K family protein
ATU_RS22165	Atu4724		CsbD family protein
ATU_RS24185	Atu5049	Ku	Ku protein
ATU_RS19335	Atu4136		ferritin-like domain-containing protein
ATU_RS22435	Atu4780		hypothetical protein
ATU_RS07400	Atu1501		hypothetical protein
ATU_RS20260	Atu4326	proP	glycine betaine/L-proline transporter ProP
ATU_RS24215	Atu5055	ligD	DNA ligase D
ATU_RS17435	Atu3751		sulfite exporter TauE/SafE family protein
ATU_RS07010	Atu1420	ligM	aminomethyltransferase family protein
ATU_RS26225	Atu5491	catE	catalase C

Fig. S17 (continued). Expression profiles of representative genes with module membership >0.9 from each WGCNA module.

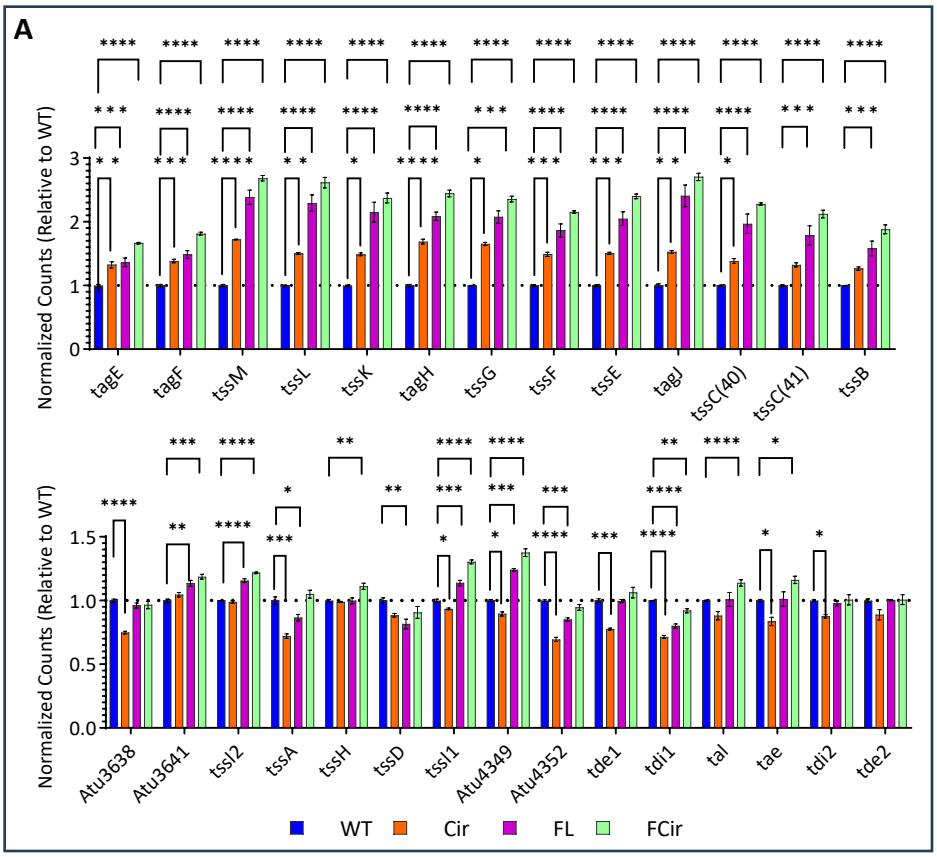

B

Gene Name*	GenBank ID	NCBI ID	Description
	Atu3638	ATU_RS26640	hypothetical protein
tdi2	Atu3639	ATU_RS16900	GAD-like domain-containing protein
tde2	Atu3640	ATU_RS16905	polymorphic toxin type 15 domain-containing protein
	Atu3641	ATU_RS16910	DUF2169 domain-containing protein
tssI2	Atu3642	ATU_RS16915	type VI secretion system tip protein TssI/VgrG
tagE	Atu4330	ATU_RS20275	protein kinase
tagF	Atu4331	ATU_RS20280	type VI secretion system-associated protein TagF
tssM	Atu4332	ATU_RS20285	type VI secretion system membrane subunit TssM
tssL	Atu4333	ATU_RS20290	type VI secretion system protein TssL, long form
tssK	Atu4334	ATU_RS20295	type VI secretion system baseplate subunit TssK
tagH	Atu4335	ATU_RS20300	type VI secretion system-associated FHA domain protein
tssG	Atu4336	ATU_RS20305	type VI secretion system baseplate subunit TssG
tssF	Atu4337	ATU_RS20310	type VI secretion system baseplate subunit TssF
tssE	Atu4338	ATU_RS20315	type VI secretion system baseplate subunit TssE
tagJ	Atu4339	ATU_RS20320	type VI secretion system accessory protein TagJ
tssC	Atu4340	ATU_RS20325	type VI secretion system contractile sheath large subunit
tssC	Atu4341	ATU_RS20330	type VI secretion system contractile sheath large subunit
tssB	Atu4342	ATU_RS20335	type VI secretion system contractile sheath small subunit
tssA	Atu4343	ATU_RS20340	type VI secretion system protein TssA
tssH	Atu4344	ATU_RS20345	type VI secretion system ATPase TssH
tssD	Atu4345	ATU_RS20350	Hcp family type VI secretion system effector
tal	Atu4346	ATU_RS20355	Rap1a/Tai family immunity protein
tae	Atu4347	ATU_RS20360	type VI secretion system amidase effector protein Tae4
tssI1	Atu4348	ATU_RS20365	type VI secretion system tip protein VgrG
	Atu4349	ATU_RS20370	DUF4123 domain-containing protein
tde1	Atu4350	ATU_RS20375	polymorphic toxin type 15 domain-containing protein
tdi1	Atu4351	ATU_RS20380	GAD-like domain-containing protein
	Atu4352	ATU_RS20385	PAAR domain-containing protein

*Note: Gene name based on annotation provided in Ma et al., 2014 (64), doi: 10.1016/j.chom.2014.06.002

Fig. S18. Transcriptome analysis of the Type VI Secretion System (T6SS) gene cluster in *Agrobacterium tumefaciens* C58 variants. (**A**) Normalized RNA-seq read counts of individual T6SS component genes across C58 variants under uninduced conditions. (**B**) Table listing functional descriptions of each T6SS gene plotted in (**A**). Error bars represent the standard error of the mean from $N = 3$ biological replicates. Asterisks denote statistically significant differences based on one-way ANOVA followed by Dunnett's multiple comparison test (****, $p < 0.0001$; ***, $p < 0.001$; **, $p \leq 0.01$; *, $p \leq 0.05$, no asterisk, not significant).

Table S1. Strains and plasmids used in this study

Strains and plasmids	Abbreviation in the text	Description	Reference
Strains			
AGL1		*recA* deficient strain derivative of AGL0 (recA::bla pTiBo542ΔT Mop^{+} Cb^{R})	94
C58	WT	Wildtype *Agrobacterium* strain obtained from Oregon State University (OSU)	18, 19
C58Cir	Cir	Cured C2 circularized chromid mutant derived from C58	This study
C58FCir-cre		Cured circularized ~4.9 Mb chromosome mutant strain derived from C58FCir	This study
C58F	FL	C1-C2 chromosomally fused strain with a large linear chromosome of ~4.9 Mb	Community source, origin unknown
C58FCir	FCir	Uncured circularized ~4.9 Mb chromosome mutant strain derived from C58F	This study
C58CirD		Mutant strain obtained by deleting ~194 kb of pAt in C58Cir	This study
C58FCir-RFP		Subtelomeric mCherry insertion mutant derived from C58FCir and used for competition assay	This study
C58Cir_ΔtelA		*telA* knockout insertion mutant derived from C58Cir	This study
C58FCir_ΔtelA		*telA* knockout insertion mutant derived from C58FCir	This study
C58-RFP		subtelomeric mCherry insertion mutant derived from C58 and used for competition assay	This study
C58Cir-RFP		subtelomeric mCherry insertion mutant derived from C58cir and used for competition assay	This study
C58F-RFP		Subtelomeric mCherry insertion mutant derived from C58F and used for competition assay	This study
C58WD		Mutant strain obtained by deleting ~194 kb of pAt in C58	This study
EHA105	E5	derivative of A281 (A136/pTiBo542)	43
EHA105 / 291A-1		subtelomeric mCherry insertion mutant derived from EHA105 and used for competition assay	This study
EHA105Cir	E5Cir	C2 circularized chromid mutant derived from EHA105	This study
EHA105Cir / 291A-1		subtelomeric mCherry insertion mutant derived from EHA105Cir and used for competition assay	This study
EHA105Cir_ΔtelA		*telA* knockout insertion mutant derived from EHA105Cir	This study
EHA105Δhom		Mutant strain obtained by deleting ~753 bp from the C2 fusion site (713,640…713,894; Accession number NC_003063)	This study
Plasmids			
pCBL101-RUBY		T-DNA binary vector for betalain biosynthesis marker *RUBY*	93
pEA106		Inducible PvirB-mCherry construct based on the PvirB promoter sequence obtained from pTiBo542	This study
pEA106c		Inducible PvirB-mCherry construct based on the PvirB promoter sequence obtained from pTiC58	This study
pEA186		INTEGRATE vector with mCherry cargo	29
pEA244		INTEGRATE vector with TtonB cargo	This study
pEA258		pVS1-based INTEGRATE vector to insert dual *loxP* sites into subtelomeric region of C2 chromid (C58) or linear chromosome (C58F)	This study
pEA286		pVS1-based INTEGRATE construct with mCherry cargo and crRNA targeting the protelomerase *Atu2523* gene.	This study

Strains and plasmids	Abbreviation in the text	Description	Reference
pEA291A		pVS1-based INTEGRATE construct with crRNA targeting the subtelomeric C2 region and used for generating RFP mutants of C58-RFP, C58Cir-RFP and C58F-RFP	This study
pEA297		pVS1-based INTEGRATE vector with a *loxP* cargo and dual crRNAs targeting the C1-C2 homology region. This construct, in conjunction with a site specific recombinase vector, was used to generate the EHA105Δhom strain	This study
pEA302		pVS1-based INTEGRATE construct with crRNA targeting the C2 *picA* (*Atu3129*) locus and used for generating the C58FCir-RFP mutant used for competition assay	This study
pEA384		Spectinomycin-based construct used to determine the essentiality of Cre recombinase to the C58FCir genome configuration.	This study
pEA385		pVS1-based INTEGRATE construct with tonB cargo and crRNA targeting the *xerC* recombinase gene	This study
pEA386		pVS1-based INTEGRATE construct with tonB cargo and crRNA targeting the *xerD* recombinase gene	This study
pEA387		pVS1-based INTEGRATE construct with tonB cargo and dual crRNA targeting the *xerC -xerD* recombinase gene	This study
pEA388		pVS1-based INTEGRATE construct with tonB cargo and crRNA targeting the *repB* partition protein encoding gene	This study
pEA389		pVS1-based INTEGRATE construct with tonB cargo and crRNA targeting the *parB* partition protein encoding gene	This study
pEA393		pVS1-based INTEGRATE construct with Cre recombinase cargo and crRNA targeting the *Atu2523* telomerase gene	This study
pEA394		Construct containing partially cloned fragments of *xerC* , *xerD* , *repB* , and *parB* . pEA394 served as the target destination to validate the functionality of the *xerC* , *xerD* , *repB* , and *parB* crRNAs	This study
pKL2299A		Ternary helper plasmid with *virA* from Bo542 Ti plasmid	44
pKL2310		Empty pVS1-based INTEGRATE vector with *loxP* cargo. Cargo can be replaced by *Pst* I and *Xho* I digestion. Dual *Bsa* I-sites for new spacer cloning.	29
pKL2315		Cre recombinase vector for targeted DNA deletion via recombination between two *loxP* sites	29

Table S2. General RNA-sequencing stats for four C58 variants

	Strain	Abbr.	Replicate	AS or DMSO	Sample Name	M Seqs	% GC	% Reads PF	% Reads Removed	% Aligned	% Dups	% rRNA	% Assigned	M Assigned	Numbers of genes detected
1	Wildtype	WT	1	AS	W1a	42.5	55%	99.50%	0.10%	92.40%	69.20%	3.44%	83.80%	35.2	5330
2	Wildtype	WT	2	AS	W2a	44.8	55%	99.50%	0.20%	92.20%	68.60%	3.35%	83.50%	36.9	5328
3	Wildtype	WT	3	AS	W3a	41.5	55%	99.50%	0.10%	92.20%	68.00%	3.66%	83.80%	34.4	5330
4	Wildtype	WT	1	DMSO	W1d	39.1	56%	99.50%	0.10%	91.30%	59.30%	4.20%	83.80%	32.4	5329
5	Wildtype	WT	2	DMSO	W2d	42	56%	99.50%	0.10%	90.90%	59.80%	4.57%	83.40%	34.7	5329
6	Wildtype	WT	3	DMSO	W3d	42.2	56%	99.50%	0.10%	91.30%	60.30%	4.25%	83.50%	34.8	5328
7	Circularized	Cir	1	AS	C1a	40.1	55%	99.50%	0.10%	91.50%	66.60%	3.21%	83.20%	32.9	5328
8	Circularized	Cir	2	AS	C2a	39.3	55%	99.50%	0.10%	91.20%	66.80%	3.38%	82.80%	32.2	5326
9	Circularized	Cir	3	AS	C3a	41.6	55%	99.40%	0.20%	91.20%	67.00%	3.20%	83.30%	34.2	5327
10	Circularized	Cir	1	DMSO	C1d	38.4	57%	99.50%	0.10%	89.70%	58.60%	5.15%	82.50%	31.3	5330
11	Circularized	Cir	2	DMSO	C2d	42.8	56%	99.50%	0.10%	88.30%	59.70%	6.52%	81.40%	34.4	5331
12	Circularized	Cir	3	DMSO	C3d	37.6	57%	99.50%	0.10%	90.80%	57.50%	4.60%	83.80%	31.1	5327
13	Fused Linear	FL	1	AS	F1a	40.5	55%	99.60%	0.10%	93.00%	65.90%	3.39%	84.70%	34	5186
14	Fused Linear	FL	2	AS	F2a	40.2	55%	99.50%	0.10%	93.70%	65.80%	2.77%	85.20%	33.9	5175
15	Fused Linear	FL	3	AS	F3a	40	56%	99.60%	0.10%	92.90%	64.80%	3.88%	84.90%	33.7	5179
16	Fused Linear	FL	1	DMSO	F1d	38.3	57%	99.40%	0.10%	93.70%	55.90%	3.79%	86.10%	32.6	5185
17	Fused Linear	FL	2	DMSO	F2d	40.5	57%	99.50%	0.10%	92.00%	57.30%	6.14%	85.10%	34.1	5184
18	Fused Linear	FL	3	DMSO	F3d	39.1	57%	99.50%	0.10%	94.50%	56.30%	3.32%	86.90%	33.7	5199
19	Fused Circularized	FCir	1	AS	FC1a	38.4	55%	99.60%	0.10%	92.40%	63.70%	2.87%	85.10%	32	5175
20	Fused Circularized	FCir	2	AS	FC2a	39.5	55%	99.60%	0.10%	93.00%	66.20%	1.95%	86.10%	33.3	5172
21	Fused Circularized	FCir	3	AS	FC3a	42.7	55%	99.60%	0.10%	92.90%	66.40%	2.40%	85.80%	35.9	5172
22	Fused Circularized	FCir	1	DMSO	FC1d	36	57%	99.50%	0.10%	91.20%	55.00%	4.31%	86.20%	30.1	5183
23	Fused Circularized	FCir	2	DMSO	FC2d	39.8	57%	99.60%	0.10%	90.00%	56.80%	5.67%	84.90%	32.9	5188
24	Fused Circularized	FCir	3	DMSO	FC3d	41.8	57%	99.60%	0.10%	92.10%	55.70%	3.17%	86.80%	35.3	5198

Table S3. List of data files from the RNAseq analysis deposited in Zenodo Repository

Name	Description
Table A1	RNAseq workflow with software versions and analysis parameters
Table A2	Summary of the DESeq2 output comparing expression of AS vs DMSO samples
Table A3	DESeq2 Fold Change and Normalized Counts (Log2 transformed)
Table A4	KEGG number assignment for ASM9202v1
Table A5	KEGG pathways of upregulated DEGs from each strain
Table A6	KEGG pathways of DEGs downregulated in each strain
Table A7	Genes in each WGCNA module, their GS and MM
Table A8	All genes in Blue module with descriptions and expression values for those with MM > 0.9
Table A9	All genes in Magenta module with descriptions and expression values for those with MM > 0.9
Table A10	All genes in Yellow module with descriptions and expression values for those with MM > 0.9
Table A11	All genes in Turquoise module with descriptions and expression values for those with MM > 0.9
	(Note: orange boxes are genes in pAt truncated region in FL and FCir and were filtered out for analysis)
Table A12	All genes in Green module with descriptions and expression values for those with MM > 0.9

Zenodo Repository ID number: 15122195

Table S4. Oligonucleotides used in this study.

Primers for cloning and sequencing

Oligonucleotide name	Description	Sequence
382-gRNA-F1	Forward oligonucleotide spacer cloned into pEA382 for targeted insertion of the pKL2315 harbored *sacB* gene. This sequence was hybridized with 382-gRNA-R1	ATAACAGTGGACGCGACGTCCGATGAAGTCAGGAAGAG
382-gRNA-R1	Reverse oligonucleotide spacer cloned into pEA382 for targeted insertion of the pKL2315 harbored sacB gene. This sequence was hybridized with 382-gRNA-F1	TTCACTCTTCCTGACTTCATCGGACGTCGCGTCCACTG
382-seq-F1	Forward sequencing primer for screening transposon insertion in the pKL2315 harboring *sacB* gene	GAGCGAAACCCTATAGGAACCC
382-seq-R1	Reverse sequencing primer for screening transposon insertion in the pKL2315 harboring *sacB* gene	TCCAAGGTGTTGCTGGATGGTC
383-gRNA-F1	Forward oligonucleotide spacer cloned into pEA383 for targeted insertion of the pKL2315 harbored cre recombinase gene. This sequence was hybridized with 383-gRNA-R1	ATAACGTCAGCGTTTTGCAGCGGCCAGCTGTCCCACAG
383-gRNA-R1	Reverse oligonucleotide spacer cloned into pEA383 for targeted insertion of the pKL2315 harbored cre recombinase gene. This sequence was hybridized with 383-gRNA-F1	TTCACTGTGGGACAGCTGGCCGCTGCAAAACGCTGACG
383-seq-F1	Forward sequencing primer for screening transposon insertion in the pKL2315 harboring *cre* recombinase gene	CGGACCATTCTTGCGTCTGATC
383-seq-R1	Reverse sequencing primer for screening transposon insertion in the pKL2315 harboring *cre* recombinase gene	TTACCCGGCCAGTACATACAGG
393-seq-F1	Forward primer used to amplify the *cre* recombinase cargo cloned into pEA393 INTEGRATE vector. This vector was used for generating the C58FCir-cre strain	GTCTAAACTTCAGTAAGTTTACGACATTTTCCTCGAGTTTACGGCTAGCTCAGCCCTAGG
393-seq-R1	Reverse primer used to amplify the *cre* recombinase cargo cloned into pEA393 INTEGRATE vector. This vector was used for generating the C58FCir-cre strain	TTTTGTGAATCGAGTATTTCAGCAAAACTACTGCAGAGTCAAAAGCCTCCGACCGGAGGC
394-seq-F1	Forward primer used to clone the pEA394 pBBR1-KanR vector backbone	CATCGAACATCGTCAAAACGATGCCCTGTATATCAAGCTGTACAGCCGATAGTCTGGAAC
394-seq-R1	Reverse primer used to clone the pEA394 pBBR1-KanR vector backbone	TAGCTACGCCGTGCCCGAGGATATGGTGGTCGAGACCGGTAATCTCGTGATGGCAGGTTG
394-seq-F2	Forward primer used to amplify a partial fragment of the *xerC* gene cloned into pEA394	GACCGACCAAGCGACGCCCAACCTGCCATCACGAGATTACCGGTCTCGACCACCATATCC
394-seq-R2	Reverse primer used to amplify a partial fragment of the *xerC* gene cloned into pEA394	ACGGGCAAAGCTCGGACGGCGCAACATCGTCTTCGTGGTCATTCAACTGTGCCTCGGCCG
394-seq-F3	Forward primer used to amplify a partial fragment of the *xerD* gene cloned into pEA394	GCGCTGAAAATCACCACGGCCGAGGCACAGTTGAATGACCACGAAGACGATGTTGCGCCG
394-seq-R3	Reverse primer used to amplify a partial fragment of the *xerD* gene cloned into pEA394	GAAGGCGCGGTTTGCCCAGAAACTGCAGATGCGGTTCCAACTGCCGCATGGAGGAGAGAC
394-seq-F4	Forward primer used to amplify a partial fragment of the *repB* gene cloned into pEA394	ACCTCGCAGGCGCGGCGTCTCTCCTCCATGCGGCAGTTGGAACCGCATCTGCAGTTTCTG
394-seq-R4	Reverse primer used to amplify a partial fragment of the *repB* gene cloned into pEA394	CGTGCAGCGTTCCGACCTCAATCCGCTTGAAGAGGCGACCACAGAACCAGATGGTCGCCT
394-seq-F5	Forward primer used to amplify a partial fragment of the *parB* gene cloned into pEA394	AAGATGGAGCGCAGGAAGGCGACCATCTGGTTCTGTGGTCGCCTCTTCAAGCGGATTGAG
394-seq-R5	Reverse primer used to amplify a partial fragment of the *parB* gene cloned into pEA394	GCAACCCGTAAGTGCGCTGTTCCAGACTATCGGCTGTACAGCTTGATATACAGGGCATCG
C58F-seq-C1F	C1-specific forward primer for confirming fusion junction for C1 and C2 chromosome/chromid in C58F via colony PCR	GCCAGTGTCGCTCTATACGC
C58F-seq-C1R	C1-specific reverse primer for confirming fusion junction for C1 and C2 chromosome/chromid in C58F via colony PCR	TCGGCTAAAGCGGGTGTTTC

Oligonucleotide name	Description	Sequence
C58F-seq-C2F	C2-specific forward primer for confirming fusion junction for C1 and C2 chromosome/chromid in C58F via colony PCR	GCTCTCAGCGACCCATCTTC
C58F-seq-C2R	C2-specific reverse primer for confirming fusion junction for C1 and C2 chromosome/chromid in C58F via colony PCR	TATGCGCCGTACAACATGGC
Fusion-seq-F1	Forward sequencing primer for screening fused C1-C2 chromosome junction sites	AGACCATGCCGAAAGGATTG
Fusion-seq-R1	Reverse sequencing primer for screening fused C1-C2 chromosome junction sites	ATACATTCCACTCCCTTGGC
Fusion-seq-R2	Reverse sequencing primer for screening fused C1-C2 chromosome junction sites	GAACCAGTTGCGCTTTGAAC
HomC2-oligoF1	*Vibrio cholerae* repeat enclosing the guide RNA forward sequence for the first targeted *lox*P insertion into the C1-C2 homology region on C2 chromid. This oligo was hybridized with HomC2-oligoR1 to generate pEA297 for multiplex gene targeting	ATAACTGTTGAGCAGGATCTCGAAGTAAGAGCACTCGGTGAACTGCCGAGTAG
HomC2-oligoR1	*Vibrio cholerae* repeat enclosing the guide RNA forward sequence for the first targeted *lox*P insertion into the C1-C2 homology region on C2 chromid. This oligo was hybridized with HomC2-oligoF1 to generate pEA258 for multiplex gene targeting	CTACCTACTCGGCAGTTCACCGAGTGCTCTTACTTCGAGATCCTGCTCAACAG
HomC2-seq-F1	Forward sequencing primer for confirming the first *lox*P insertion into the homology region on C2 chromid	CTGGAAAACAGCAAGCCCAC
HomC2-seq-R1	Reverse sequencing primer for confirming the first *lox*P insertion into the homology region on C2 chromid	CGGAAACAACGCTAGCACAG
HomC2-oligoF2	*Vibrio cholerae* repeat enclosing the guide RNA forward sequence for the second targeted *lox*P insertion into the C1-C2 homology region on C2 chromid. This oligo was hybridized with HomC2-oligoR2 to generate pEA297 for multiplex gene targeting	GTAGCTGATAACAACTGATGTCATGACGACGATCTGTTTCGCGCG
HomC2-oligoR2	*Vibrio cholerae* repeat enclosing the guide RNA forward sequence for the second targeted *lox*P insertion into the C1-C2 homology region on C2 chromid. This oligo was hybridized with HomC2-oligoF2 to generate pEA297 for multiplex gene targeting	TTCACGCGCGAAACAGATCGTCGTCATGACATCAGTTGTTATCAG
HomC2-seq-F2	Forward sequencing primer for confirming the second *lox*P insertion into the homology region on C2 chromid	GAAATGCCGACGCTTGTTCC
HomC2-seq-R2	Reverse sequencing primer for confirming the second *lox*P insertion into the homology region on C2 chromid	CTGACCTCCAACGCAACCTC
INT6-oligoF	*Vibrio cholerae* repeat enclosing the guide RNA forward sequence for the first targeted *lox*P insertion into the C2 subtelomeric region. This oligo was hybridized with INT6-oligoR to generate pEA258 for multiplex gene targeting	ATAACTCATCAGGGCGGTATCTGCACGAGTAGCAAGGGTGAACTGCCGAGTAG
INT6-oligoR	*Vibrio cholerae* repeat enclosing the guide RNA reverse sequence for first targeted *lox*P insertion into the C2 subtelomeric region. This oligo was hybridized with INT6-oligoF to generate pEA258 for multiplex gene targeting	CTACCTACTCGGCAGTTCACCCTTGCTACTCGTGCAGATACCGCCCTGATGAG
INT6-seq-F1	Forward sequencing primer for confirming the first *lox*P insertion into the subtelomeric region on C2 chromid	CCGATTTCGAAGCTTTGCCC
INT6-seq-R1	Reverse sequencing primer for confirming the first *lox*P insertion into the subtelomeric region on C2 chromid	CAGGTAAAGTCCTCTGGCCG
INT7-oligoF	pEA258 *Vibrio cholerae* repeat enclosing the guide RNA forward sequence for the second targeted *lox*P insertion into the C2 subtelomeric region. This oligo was hybridized with INT7-oligoR for multiplex gene targeting	GTAGCTGATAACAATTCTATCGCGACGAGAGCAGTACGCGCTGCG
INT7-oligoR	*Vibrio cholerae* repeat enclosing the guide RNA reverse sequence for the second targeted *lox*P insertion into the C2 subtelomeric region. This oligo was hybridized with INT7-oligoF to generate pEA258 for multiplex gene targeting	TTCACGCAGCGCGTACTGCTCTCGTCGCGATAGAATTGTTATCAG

Oligonucleotide name	Description	Sequence
INT7-seq-F1	Forward sequencing primer for confirming the second *lox*P insertion into the subtelomeric region on C2 chromid	GAGCTTTCGTGAGCGTTTCC
INT7-seq-R1	Reverse sequencing primer for confirming the second *lox*P insertion into the subtelomeric region on C2 chromid	CAAACCACCCACTCACCCTC
INT10-oligoF1	Forward oligonucleotide spacer cloned into pEA291A for targeted mCherry insertion into the C2 subtelomeric region of C58, C58Cir, and C58F	ATAACGCAGGCATTCATTAAAGCGTTCTGGCGACATGG
INT10-oligoR1	Reverse oligonucleotide spacer cloned into pEA291A for targeted mCherry insertion into the C2 subtelomeric region of C58, C58Cir, and C58F	TTCACCATGTCGCCAGAACGCTTTAATGAATGCCTGCG
INT10-seq-F1	Forward sequencing primer for confirming mCherry insertion into the subtelomeric region on C2 chromid of C58, C58Cir, and C58F	GCTTTCGTGAGCGTTTCCAG
INT10-seq-R1	Reverse sequencing primer for confirming mCherry insertion into the subtelomeric region on C2 chromid of C58, C58Cir, and C58F	AATATTCCACCTGCGCACC
LoxP-R1	*lox*P-*specific* primer combined with colony PCR primers to validate Tn orientation after targeted insertion	CCTCGAGGTCATTTCATAAC
picA-oligoF	Forward oligonucleotide spacer cloned into pEA302 for targeted mCherry insertion into the *picA* locus of C58FCir	ATAACGGCAGGTGATAGCGCGCATCTGGTGCGGCAAGG
picA-oligoR	Reverse oligonucleotide spacer cloned into pEA302 for targeted mCherry insertion into the *picA* locus of C58FCir	TTCACCTTGCCGCACCAGATGCGCGCTATCACCTGCCG
picA-seq-F1	Forward sequencing primer for confirming mCherry insertion into the C2 *picA* locus of C58FCir	AATTCCAGACTGCCGAACCC
picA-seq-R1	Reverse sequencing primer for confirming mCherry insertion into the C2 *picA* locus of C58FCir	TGAACATCCGGAAATCCGCT
PvirB-pTiC58-F1	Forward primer to amplify the pTiC58-specific *virB* promoter cloned into pEA106c	GGGGTACCTTTCAGGAGACTCGACCAGG
PvirB-pTiC58-R1	Reverse primer to amplify the pTiC58-specific *virB* promoter cloned into pEA106c	CGGAATTCTCCCCATCTCCCCAAGCTCATAAC
telA-oligo-F1	Forward oligonucleotide spacer cloned into pEA286 for targeted insertion of the a*tu2523 (telA)* gene. This sequence was hybridized with telA-oligoR1.	ATAACAGATCAAAGAGGCGATGAAAAGCGACGACGCTG
telA-oligo-R1	Reverse oligonucleotide spacer cloned into pEA286 for targeted insertion of the a*tu2523 (telA)* gene. This sequence was hybridized with telA-oligoF1.	TTCACAGCGTCGTCGCTTTTCATCGCCTCTTTGATCTG
telA-seq-F1	Forward sequencing primer for confirming mCherry insertion into the protelomerase a*tu2523 (telA)* gene.	TCATCACATTCCCGCAACCG
telA-seq-R1	Reverse sequencing primer for confirming mCherry insertion into the protelomerase *atu2523 (telA)* gene	GGCTATGCGAAGGAGAACCG

Primers for RT-qPCR

Oligonucleotide name	Description	Sequence
ChvG-seq-F3	Forward primer to amplify chromosomal *chvG* gene.	GGTATCGACCGATGCGGAA
ChvG-seq-R3	Reverse primer to amplify chromosomal *chvG* gene.	ACCTCAACCAGTTCCGTGAAG
ChvI-seq-F3	Forward primer to amplify chromosomal *chvI* gene.	CGGCTTTGTGATGAAATCGTCT
ChvI-seq-R3	Reverse primer to amplify chromosomal *chvI* gene.	ATTCCCGTTATCTTCCTCACCTC
rpoD-C1-set1F	Forward primer to amplify the house keeping sigma factor *rpoD* gene used as an internal reference control for qPCR.	CCATCTCCTTCTTGGCGATAC
rpoD-C1-set1R	Reverse primer to amplify the house keeping sigma factor *rpoD* gene used as an internal reference control for qPCR.	GTCAGGAAATCCAGAACCTCTC
virA-seq-F2	Forward primer to amplify pTiC58 *virA* gene.	ACCGCTGAAATTGCCGAAAG
virA-seq-R2	Reverse primer to amplify pTiC58 *virA* gene.	ACGGAACCCAAGAAGATCCG
virB1-seq-F2	Forward primer to amplify pTiC58 *virB1* gene.	GAACGGCTACGTGCGAAAAG
virB1-seq-R2	Reverse primer to amplify pTiC58 *virB1* gene.	ATCCCGGCTTCTCACGATCA
virC1-seq-F2	Forward primer to amplify pTiC58 *virC1* gene.	CGGAGTTAACATGGTCGGGA
virC1-seq-R2	Reverse primer to amplify pTiC58 *virC1* gene.	ATTATGCGCTGGCCGATACG
virD2-seq-F2	Forward primer to amplify pTiC58 *virD2* gene.	CAATCGGCAGAATGAGTCGC
virD2-seq-R2	Reverse primer to amplify pTiC58 *virD2* gene.	TCCGTCTCCAATGCAACCC
virE2-seq-F3	Forward primer to amplify pTiC58 *virE2* gene.	CCTGGAGCCAAGAGAACAGAG
virE2-seq-R3	Reverse primer to amplify pTiC58 *virE2* gene.	AGATGTCGGTGCCAGTGATG
virG-seq-F2	Forward primer to amplify pTiC58 *virG* gene.	GCGAACCAAAGATCGACGCT
virG-seq-R2	Reverse primer to amplify pTiC58 *virG* gene.	GTTTCACCTCACTGCCCTCT

Table S5. Hi-C sequencing summary statistics

Sample ID	Genotype	Valid Pairs	% Valid	Mapped Side 1	Total Reads
AtWX769_ATGN_rep1	C58_rep1	11397552	30.3%	36493303	37556247
AtWX769_ATGN_rep2	C58_rep2	13647292	34.9%	37780883	39091233
AtWX771_ATGN_rep1	C58Cir_rep1	13176955	35.4%	35858332	37194804
AtWX771_ATGN_rep2	C58Cir_rep2	9444717	26.9%	34074844	35096302
AtWX773_ATGN_rep1	C58F_rep1	11389366	34.0%	32414953	33467742
AtWX773_ATGN_rep2	C58F_rep2	10452779	35.0%	28918364	29881267
AtWX775_ATGN_rep1	C58FCirA_rep1	11798656	37.1%	30808845	31783684
AtWX775_ATGN_rep2	C58FCirA_rep2	10572446	29.4%	34867880	35911358
AtWX777_ATGN_rep1	C58FCirB_rep1	14328412	39.7%	34742164	36111864
AtWX777_ATGN_rep2	C58FCirB_rep2	12917939	31.2%	40138058	41378502

Table S6. RT-qPCR primer efficiency

Target Gene	Location	Primer (forward/reverse)	R^2	Slope	Efficiency (%)	Amplification factor (where 2 = 100%)
rpoD	C1 chromosome	rpoD-C1-set1F/R	0.9999	-3.1195	109.20	2.092
chvG	C1 chromosome	ChvG-seq-F3/R3	0.9984	-3.2965	101.07	2.011
chvI	C1 chromosome	ChvI-seq-F3/R3	0.9998	-3.3525	98.74	1.987
virA	pTiC58	virA-seq-F2/R2	0.9899	-3.315	100.29	2.003
virB1	pTiC58	virB1-seq-F2/R2	0.9857	-3.172	106.66	2.067
virC1	pTiC58	virC1-seq-F2/R2	0.9863	-3.3415	99.19	1.992
virD2	pTiC58	virD2-seq-F2/R2	0.988	-3.275	102.00	2.020
virE2	pTiC58	virE2-seq-F3/R3	0.9993	-3.1705	106.73	2.067
virG	pTiC58	virG-seq-F2/R2	0.9869	-3.1565	107.40	2.074